JOINT EUROPEAN TORUS JET

JET–P(89)22

B. Coppi, S. Migliuolo
and JET Team

Global Modes and High Energy Particles in Ignited Plasmas

"This document contains JET information in a form not yet suitable for publication. The report has been prepared primarily for discussion and information within the JET Project and the Associations. It must not be quoted in publications or in Abstract Journals. External distribution requires approval from the Publications Officer, JET Joint Undertaking, Abingdon, Oxon, OX14 3EA, UK".

"Enquiries about Copyright and reproduction should be addressed to the Publications Officer, EFDA, Culham Science Centre, Abingdon, Oxon, OX14 3DB, UK."

The contents of this preprint and all other JET EFDA Preprints and Conference Papers are available to view online free at www.iop.org/Jet. This site has full search facilities and e-mail alert options. The diagrams contained within the PDFs on this site are hyperlinked from the year 1996 onwards.

Global Modes and High Energy Particles in Ignited Plasmas

B. Coppi, S. Migliuolo
and JET Team*

JET-Joint Undertaking, Culham Science Centre, OX14 3DB, Abingdon, UK

Massachusetts Institute of Technology, Cambridge, Massachusetts 02319, USA
** See Appendix 1*

Preprint of Paper to be submitted for publication in
Physics of Fluids

ABSTRACT.

Fusion produced alpha particles may spontaneously enhance the stability of an ignited plasma against m = 1 internal modes. Stable values of the peloidal beta of the thermal plasma component significantly in excess of the ideal MHD threshold can be attained, provided the region where the magnetic helical parameter q is below unity is not too wide and the ignition temperature is not too high. A comprehensive analysis of the different instability regimes is presented, with special attention to so-called "fishbone oscillations" and their influence on the ignition energy balance. The theoretical predictions compare favourably with sawtooth suppression experiments in JET with high power ion cyclotron resonant frequency heating, where energetic ions in the MeV range are produced.

I INTRODUCTION

One of the goals of ignition experiments is to reach the conditions where the plasma heating provided by the charged fusion reaction products can compensate for all forms of energy loss. In particular, if we refer to a Deuterium-Tritium (DT) plasma mixture, relevant questions are whether the 3.5MeV alpha particles produced by the DT reactions can be confined within the plasma column for the duration of their slowing down and, if confined, whether they will affect the plasma stability and energy transport. The classical aspects of the energetic particle confinement, namely 'prompt' losses due to intersection of their orbits with the wall of the vessel, as well as classical diffusion across the magnetic field, 'ripple losses' etc. have been extensively investigated (see e.g. Ref.[1] and references therein and more recently Ref.[2]). These problems are to a great extent solvable by optimising the machine parameters, most notably the plasma current, and will not be addressed here. From the point of view of stability, the effect of the energetic particles produced by the fusion reactions on short wave length modes, such as ballooning modes, has also received vast attention in the last decade (see e.g. Refs.[3-7]).

The aim of the present paper is to examine the role that the fusion produced particles will play on the stability of global modes in an ignited or igniting plasma. In particular we will consider the oscillations of the central part of the plasma column. These 'sawtooth' and 'fishbone' oscillations, as they are dubbed, are considered to be a potential threat to the attainment of ignition conditions: they could either cause too frequent a relaxation of the central plasma temperature or spoil the confinement of the fusion products in the central region of the plasma where the energy they deposit is needed in order to sustain the fusion reactions.

Recent experiments have shown that high energy particles can indeed significantly influence the stability of global modes. In the JET experiment, the internal relaxation oscillations of the electron temperature have been suppressed for periods of up to 3.2s during intense auxiliary heating [8]. These sawtooth-free discharges are characterised by the presence of anisotropic (mostly trapped) high energy ions, accelerated by radio frequency fields at the ion cyclotron resonance, and/or produced by neutral beam injection. On the other hand, bursts of fishbones oscillations (after the characteristic signature of the detected magnetic fluctuations), associated with the loss of high energy ions, were first discovered in the Poloidal Divertor Experiment (PDX) at Princeton during high beta operation with beams of fast neutrals injected at a quasi-perpendicular angle with respect to the toroidal magnetic field [9]. Fishbone oscillations were later found to occur in a number of experimental devices under varying conditions, including quasi-tangential beam injection [10] and occasionally, although in a milder form, in beam-heated discharges in the Tokamak Fusion Test Reactor (TFTR) at Princeton [11], and during ion cyclotron heating in JET [12].

Sawtooth suppression by energetic particles [13] and fishbone oscillations [14,15] are intrinsically related phenomena. They can be described in terms of a single dispersion relation, as they arise from the reactive part and from the dissipative (resonant) part respectively of the kinetic, as opposed to fluid, response of the high energy particle population to magnetohydrodynamic (MHD) internal oscillations. In order to illustrate this point we refer to the well known dispersion relation of internal "kink" modes. In an axisymmetric toroidal configuration these have $n = 1$ toroidal mode number and are dominated by the poloidal harmonic corresponding to $m = 1$. If we omit at first dissipation and energetic particle effects, but retain the thermal ion diamagnetic contribution, this dispersion relation is quadratic in the mode frequency and takes the form [16,17]

$$[\omega(\omega - \omega_{di})]^{1/2} = i\gamma_{mhd} \equiv i\omega_A \lambda_H. \qquad (1)$$

Here, ω is the mode frequency in the plasma rest frame, $\omega_{di} = [(k_\theta c/enB)(dp_i/dr)]_o$ is the ion diamagnetic frequency evaluated at the surface $r = r_o$ where the magnetic helical parameter $q(r) = (2\pi)^{-1} \int(\bar{B}\cdot\nabla\zeta)/(\bar{B}\cdot\nabla\theta)\, d\theta$ equals unity, r is a generalised radial coordinate which labels the nested magnetic surfaces, ζ and θ are the toroidal and generalised poloidal angles respectively, $k_\theta \simeq -1/r$, and p_i is the thermal ion pressure. The ideal MHD growth rate γ_{mhd}, obtained from (1) in the limit $\omega_{di} \to 0$, is expressed in terms of the product of the Alfvén frequency, $\omega_A = V_A/R_o\sqrt{3}$, with $V_A = (B^2/4\pi\rho_m)^{1/2}$, ρ_m is the mass density, and R_o the torus major radius, multiplied by the ideal MHD driving term, λ_H. This is related [17] to the negative of the ideal MHD energy functional δW and is of order $(\epsilon_o \beta_p)^2$, where $\epsilon_o \equiv r_o/R_o$ is the inverse aspect ratio at the q = 1 surface and β_p is the plasma poloidal beta. The dispersion relation (1) is valid for $\lambda_H > 0$: in the absence of resistivity, this condition guarantees the spatial regularity of the perturbed plasma displacement across the q = 1 surface. Positive values of λ_H are obtained when β_p is larger than a threshold value $\beta_{p,mhd}$ [18] which depends on the q profile and on the shape of the magnetic surfaces [19]. Such values are often reached in the ion-cyclotron resonant frequency (ICRF) heated sawtooth free regimes in JET when the total plasma current $I_p \lesssim 3$ MA, and are likely to be attained in ignited plasmas.

For $\gamma_{mhd} > \omega_{di}/2$, Eq.(1) gives a growing and a damped mode. The growing mode reduces to the ideal MHD internal m = 1 mode for $\gamma_{mhd} >> \omega_{di}$. The two modes coalesce for $\gamma_{mhd} = \omega_{di}/2$ and then split into two purely oscillatory modes. When $\omega_{di}/2 > \gamma_{mhd}$, the plasma stability depends on the effects of finite electrical resistivity and of the relevant mode-fast particle resonance. The latter plays the role of an effective viscosity [14]. For vanishing resistivity the stability threshold is $\lambda_H = 0$. The lower frequency

mode ($\omega < \omega_{di}/2$) is destabilised by resistivity and extends to negative values of λ_H. This mode, generally referred to as resistive internal m = 1 mode [16,17], is believed to cause, through its nonlinear development, the collapse phase of sawtooth oscillations in low β_p, collisional plasmas. However, when $\lambda_H \lesssim 0$, the stability of this branch can no longer be described by Eq.(1). Then, as will be shown in Section III-C, if resistivity is low, a regime can be entered where a proper description of the physics in the layer around the q = 1 surface leads to linear stability. Resistivity is indeed very small in an igniting plasma, and on this basis it will be neglected in the bulk of the paper.

For the relatively large values of β_p that are expected in an ignited plasma, the higher frequency branch with $\omega > \omega_{di}/2$ is of more concern. When resistivity is negligible, this branch connects to the ideal MHD internal m = 1 mode as γ_{mhd} is raised. For $\omega_{di}/2 > \gamma_{mhd}$, the mode has been shown [14] to be driven unstable by the resonant interaction with magnetically trapped energetic ions with bounce averaged magnetic drift frequency $\omega_{Dh}^{(o)}$ equal to ω. The scattering of the resonant energetic ions out of the central region of the plasma column appears as a natural by-product of this instability. The full fishbone cycle has been described [14] in terms of a simple non-linear model, whereby the mode saturates and is resistively damped once the number of resonanting particles that are being scattered has dropped sufficiently.

The above picture in terms of a higher and of a lower frequency branch remains essentially valid when the full response of the energetic particles is properly included in the dispersion equation (1). This was shown by the analyses of Refs.[13] and [14], which addressed the strongly anisotropic case where $p_{\|h}/p_{\perp h} \sim \epsilon_o$ applicable to quasi-perpendicular neutral beam injection and ICRF heating schemes. Here, $p_{\|h}$ and $p_{\perp h}$ are the components of the fast

ion pressure tensor parallel and transverse to the confining magnetic field, respectively, and we shall use the subscript "h" to indicate a generic fast ion population. The focus of this paper is on isotropic fast ion distributions, as is the case for the alpha particles produced in a DT ignited plasma. The basic features of the dispersion relation are however preserved in both cases [20,21]. This is modified into

$$[\omega(\omega - \omega_{di})]^{1/2} = i\omega_A[\lambda_H + \lambda_K(\omega)], \tag{2}$$

where the complex function $\lambda_K(\omega)$ represents the contribution of the high energy population.

The real and imaginary parts of λ_K correspond to the reactive and to the dissipative fast ion responses. The sign of Re λ_K can be related to that of the work against the perturbed energetic particle current along the perturbed electric field. Using their momentum conservation equation, this work can be rewritten in the form $-\text{Re}\ \bar{\xi}^* \cdot \nabla \cdot \overleftrightarrow{\tilde{P}}_h$, while $-\text{Im}\ \bar{\xi}^* \cdot \nabla \cdot \overleftrightarrow{\tilde{P}}_h$ expresses the dissipated energy, and $\lambda_K \propto -\int d^3x\ \bar{\xi}^* \cdot \nabla \cdot \overleftrightarrow{\tilde{P}}_h$. Here, $\bar{\xi}$ is the lowest order plasma displacement, solution of the normal mode equation, and $\overleftrightarrow{\tilde{P}}_h$ the perturbed energetic particle pressure tensor (see next section). When $\lambda_K(\omega)$ is included in the mode energy balance (see e.g. [22]), the change in the energy available to the modes is represented by the substitution $\lambda_H \rightarrow \lambda_H + \text{Re}\ \lambda_K(\omega)$.

For frequencies $\omega \ll \bar{\omega}_{Dh}$, with $\bar{\omega}_{Dh}$ a characteristic value of $\omega_{Dh}^{(o)}$, Re $\lambda_K(\omega)$ is negative. This leads to a reduction of the total instability drive. By order of magnitude, $\lambda_K \sim \epsilon_o^{3/2} \beta_{ph}$ for isotropic fast ion distributions, where β_{ph} is the energetic ion poloidal beta. This is to be compared with λ_K

$\sim \epsilon_o \beta_{ph}$ in the strongly anisotropic limit where most fast ions are trapped, the difference in the factor $\epsilon_o^{1/2}$ between the two cases being the ratio of trapped to circulating particles for an isotropic distribution. The energetic ion contribution becomes important when $\lambda_K \sim \lambda_H$. Thus the ordering relevant to the present analysis is

$$\beta_{p\alpha} \sim \epsilon_o^{1/2} \beta_p^2, \tag{3}$$

where the subscript "α" now refers to the isotropic fusion alphas. The stability condition in the absence of resistivity is modified into $\lambda_H + \mathrm{Re}\ \lambda_K(\omega) < 0$. Since, at small values of $\beta_{p\alpha}$, for both roots ω is at most of order ω_{di}, and since typically $\omega_{di}/\bar{\omega}_{D\alpha} \lesssim 10^{-1}$ in the proposed ignition experiments, we can estimate $\mathrm{Re}\ \lambda_K(\omega) \approx \lambda_K(0) = - C\epsilon_o^{3/2} \beta_{p\alpha}/s_o$, where C is a numerical factor of order unity (see Appendix) and $s_o \equiv r_o q'(r_o)$. The modified stability criterion at small $\beta_{p\alpha}$ then reads

$$\lambda_H \lesssim C\epsilon_o^{3/2} \beta_{p\alpha}/s_o. \tag{4}$$

Note that Eq.(4) does not involve the thermal-ion diamagnetic frequency ω_{di}. We recall that, in the strongly anisotropic case $p_{\|h} \sim \epsilon_o p_{\perp h}$, C is reduced by a factor $\langle 1-q \rangle$, where the brackets indicate an average over the volume within the q=1 surface. In fact, the trapped particle pressure response to a zero frequency perturbation vanishes with the parallel wave vector $k_\| \sim (1-q)/R_o$ [13,23]. If $\langle 1-q \rangle$ is smaller than $\omega_{di}/\bar{\omega}_{Dh}$, the approximation $\lambda_K(\omega) \approx \lambda_K(0)$ for the frequencies corresponding to the two branches of Eq.(1) is no longer appropriate. A term linear in $\omega/\bar{\omega}_{Dh}$ must be retained. As a consequence, the stability condition becomes dependent on the thermal-ion diamagnetic frequency in the strongly anisotropic limit [13,20].

To satisfy the stability condition (4), values of $\beta_{p\alpha}$ in excess of a finite threshold are needed. When $\beta_{p\alpha}$ is below this threshold, the type of instability will depend on ω_{di}. If $\omega_{di}/\omega_A < 2[\lambda_H + \lambda_K(0)]$, the internal $m = 1$ mode will grow on an MHD time scale. If the opposite inequality holds, then fishbone oscillations with $\omega \sim \omega_{di}$ will be excited [14]. However, as pointed out in Ref.[21], only the alpha particles that have slowed down to energies of the order of 300-400 keV can resonantly destabilise this mode. The fraction of alpha particle heating power that is lost as a consequence of the scattering of the resonating alphas is estimated to be at most a few percent. Thus, these fishbone modes do not appear to have serious consequences. On the contrary, their onset may serve the purpose of expelling the trapped alpha particles after most of their energy has been deposited, thus easing the problem of ash accumulation.

At larger values of $\beta_{p\alpha}$, $|\lambda_K| > \lambda_H$ and the higher frequency branch of Eq.(1) is significantly modified. Its frequency increases with $\beta_{p\alpha}$ and becomes comparable with $\bar{\omega}_{D\alpha}$ for values of $\beta_{p\alpha} \sim s_o \epsilon_o^{-3/2} (\bar{\omega}_{D\alpha}/\omega_A)$. When $\omega/\bar{\omega}_{D\alpha} \gtrsim 1$, the real part of λ_K becomes positive and the reactive response of the energetic alphas becomes destabilising. Then, an $m = 1$ instability entirely supported by the alpha particles becomes possible. This mode, discussed in Ref.[15], was also proposed as a candidate to explain the original observation of fishbone oscillations in the presence of energetic beam ions in PDX. This instability should be of more direct concern for the attainment of ignition condition. In fact, it would scatter newly born alpha particles carrying an energy $\epsilon \sim \epsilon_\alpha = 3.5$ MeV, and significantly affect the ignition energy balance. Under certain conditions, this scattering would however be beneficial as it could help to prevent the fusion thermal runaway.

We find that for parameters that are relevant to proposed ignition

experiments, there exists a stable interval of values of $\beta_{p\alpha}$. In addition we find that the maximum stable value of β_p is characteristically given by

$$\beta_{p,max} \simeq 0.9 \frac{[n_{io}/10^{15}cm^{-3}]^{1/4}}{(6r_o/R_o)^{3/2}(R_o/1.2m)^{1/2}(B/10^5G)}, \qquad (5)$$

with n_{io} the thermal ion density at $r = r_o$.

The existence of this stability window was first reported in Ref. [24], in a preliminary analysis of alpha particle effects on $m^0 = 1$ modes. This discovery stimulated the work which led us to propose [25,13] an explanation for the suppression of sawteeth in JET auxiliary heated discharges.

Partly similar approaches have been followed in Refs.[26] and [27]. In Refs.[26], the conclusion was drawn that values of β_p in excess of $\beta_{p,mhd}$ are needed to suppress the resistive branch. This conclusion follows primarily from the use of a model where the low frequency energetic ion response is negligible ($\lambda_K(0) \simeq 0$), and differs from the results of the present analysis (see Sec. III-c). In addition, Refs.[26] lack the recognition of the existence of the low-β_{ph} fishbone regime with $\omega \sim \omega_{di}$.

Both the maximum stable poloidal beta in Eq.(5) and the $\beta_{p\alpha}$-threshold for the excitation of high frequency ($\omega \sim \bar{\omega}_{D\alpha}$) modes scale as strong inverse powers of the radius r_o of the $q = 1$ surface. Consequently, the stable domain in the $(\beta_p, \beta_{p\alpha})$ plane is considerably reduced if the area of the plasma cross-section where q is below unity is large (say $r_o \gtrsim 0.5a$, with a the mean radius of the plasma column). Therefore, it becomes difficult for the alpha particles to suppress sawteeth and fishbones when β_p exceeds $\beta_{p,mhd}$ and the $q = 1$ radius is large.

A reduction of the stable domain also occurs in the so-called "ion-kinetic" regime [28]. This regime corresponds to large thermal ion

gyroradii, $\rho_i/r_o > \lambda_H$, and is expected to be approached or indeed entered by some of the presently planned ignition experiments. Large thermal-ion gyroradius effects are more important on the modes oscillating with frequency $\omega \sim \omega_{di}$ and are found to be destabilising. A novel result of our analysis [29] is that in the ion-kinetic regime fishbone modes with $\omega \sim \max\{\omega_{di}, (\rho_i/r_o)\omega_A\}$ can be excited even at values of β_p below the ideal MHD threshold for instability, extending the instability domain obtained in the fluid thermal ion limit [14]. Similar results have been obtained numerically in Ref.[27].

This paper is organised as follows. Section II describes the alpha-particle response to m=1 perturbations. The dispersion relation and stability criteria are discussed in general terms in Section III, while in Section IV their dependence on plasma parameters such as β_p, $\beta_{p\alpha}$, and r_o is shown explicitly. The extension of these results to the ion-kinetic regime is discussed in Section V. Finally, our conclusions are presented in Section VI.

II ALPHA PARTICLE RESPONSE AND THE OUTER REGION

The derivation of the dispersion relation for $m^0 = 1$ modes in a toroidal axisymmetric plasma in the presence of energetic particles follows the standard technique outlined in Refs.[16] and [30]. The mode structure is characterised by the presence of a transition layer of thickness δ, centred around the surface $r = r_o$ [$q(r_o) = 1$], where inertial as well as non-ideal (such as resistive) effects become important. Away from this layer the core plasma motion is governed by the ideal MHD equations. The thickness of the layer is characteristically smaller than the size of the orbits of the energetic particles. Their contribution is therefore important only in the "outer region", (that is, outside the transition layer) where it is obtained from a kinetic treatment. The dispersion relation is obtained by matching the solution of the normal mode equation in the transition layer to the outer solution. The existence of a transition layer relies on the implicit assumption that the magnetic shear is finite within the volume enclosed by the $q = 1$ surface.

In this section we evaluate the kinetic alpha-particle contribution in the outer region explicitly. The alpha particle pressure tensor $\overleftrightarrow{P}_\alpha$ is included in the momentum balance equation,

$$0 = - \nabla\tilde{p} - \nabla\cdot\tilde{\overleftrightarrow{P}}_\alpha + \frac{1}{4\pi}\,[(\nabla \times \bar{B}) \times \tilde{\bar{B}} + (\nabla \times \tilde{\bar{B}}) \times \bar{B}], \tag{6}$$

where the inertial term is neglected. A tilde indicates perturbed quantities. The perturbed thermal plasma pressure and magnetic field can be expressed in terms of the displacement vector $\bar{\xi}$ through

$$\tilde{p} = - \bar{\xi}\cdot\nabla p - (5/3)p\,\nabla\cdot\bar{\xi}, \tag{7}$$

$$\tilde{\bar{B}} = \nabla \times (\bar{\xi} \times \bar{B}). \tag{8}$$

We adopt a standard expansion in powers of $\epsilon_o \equiv r_o/R_o$. To leading order, the structure of the displacement is dominated by its m = 1 component, which can be written as

$$\bar{\xi} = \hat{\bar{\xi}}(r) \exp(-i\omega t + iR), \quad R = \zeta - \theta. \tag{9}$$

Within this expansion procedure, we may disregard the effect of the energetic alpha particles on the satellite ($m \neq 1$) poloidal harmonics. The latter are however included in the thermal plasma response. The tensor $\tilde{\overleftrightarrow{P}}_\alpha$ is obtained by taking the appropriate moment of the perturbed alpha particle distribution. This can be conveniently split in two parts,

$$\tilde{f}_\alpha = \tilde{f}_\alpha^{ad} + \tilde{f}_\alpha^{nad}. \tag{10}$$

The "adiabatic" part for $\tilde{E}_{||} = 0$ is simply

$$\tilde{f}_\alpha^{ad} = - \bar{\xi}_\perp \cdot \nabla F_{o\alpha}, \tag{11}$$

with $F_{o\alpha} = F_{o\alpha}(r,\epsilon)$ the isotropic equilibrium alpha particle distribution and $\epsilon = m_\alpha v^2/2$. For $\omega < \omega_{b\alpha}$, with $\omega_{b\alpha}$ the alpha particle bounce frequency, the non-adiabatic part, to lowest order in ϵ_o, is constant along the particle orbits and is contributed by the trapped alphas only. As shown in the Appendix, it is given by $\tilde{f}_\alpha^{nad} = \hat{f}_\alpha^{nad} \exp(-i\omega t + iS)$, where $S = (\zeta - q\theta)$ and

$$\hat{f}_\alpha^{nad} = \frac{\hat{\xi}_r}{R_o} \frac{\omega - \omega_{*\alpha}^T}{\omega - \omega_{D\alpha}^{(o)}} \epsilon \frac{\partial F_{o\alpha}}{\partial \epsilon} [\cos(q\theta)]^{(o)}. \tag{12}$$

In this equation, $(\partial F_{o\alpha}/\partial\epsilon)\ \omega_{*\alpha}^T = -\ \bar{e}_{||} \times \nabla F_{o\alpha} \cdot \nabla R/(m_\alpha\ \Omega_\alpha)$, $\omega_{D\alpha} = \bar{v}_{D\alpha} \cdot \nabla S$,

$$\bar{v}_{D\alpha} = \frac{2\epsilon}{m_\alpha \Omega_\alpha} \bar{e}_{||} \times \left[\left(1 - \frac{\Lambda}{H} \right) \bar{\kappa} + \frac{\Lambda}{2H} \frac{\nabla B}{B} \right], \tag{13}$$

$\Omega_\alpha = 2eB/m_\alpha c$, $\bar{e}_{||} = \bar{B}/B$, $\bar{\kappa} = (\bar{e}_{||} \cdot \nabla)\ \bar{e}_{||}$, $H(r,\theta) = B_o/B$ with B_o the strength of $\bar{B}$ on the magnetic axis, and $\Lambda = \mu B_o/\epsilon$ is the pitch angle in velocity space, with $\mu = m_\alpha\ v_\perp^2/2$. The superscript (o) indicates averaging over bounce orbits, that is $A^{(o)} = (\int A\ d\ell/|v_{||}|)/(\int d\ell/|v_{||}|)$, with ℓ the coordinate along a field line. For modes with frequencies $\omega \sim \bar{\omega}_{D\alpha}$ we can neglect ω in the numerator of (12) since it is one order higher in ϵ_o compared with $\omega_{*\alpha}^T$.

Equations (6)-(8) can be reduced to a single equation for the m = 1 component of the radial displacement ξ_r. To leading order in ϵ_o, we find $\xi_r = \Theta(-z)\ \xi_o$, where ξ_o is a constant, $z \equiv (r - r_o)/r_o$, and $\Theta(z)$ is the Heaviside function. To the next relevant order we obtain, as $r \to r_o$,

$$\frac{d\hat{\xi}_r}{dz}\ \underset{z \to 0}{\sim}\ - \frac{\lambda_H + \lambda_K(\omega)}{\pi\ s_o\ z^2}\ \hat{\xi}_o. \tag{14}$$

We recall that $\lambda_H \sim (\epsilon_o\ \beta_p)^2$. The instability condition in the ideal MHD approximation, $\lambda_H > 0$, is satisfied when β_p exceeds a critical threshold, $\beta_{p,mhd}$. The appropriate expression for the poloidal beta is

$$\beta_p = \frac{8\pi}{B_p^2(r_o)} [\langle p(r_o) \rangle - p(r_o)], \tag{15}$$

with $\langle p(r_o)\rangle$ the average of p within the volume enclosed by the q=1 surface. The exact value of $\beta_{p,mhd}$ is determined by the shape of the q profile and of the plasma cross-section, and varies characteristically between 0.1 and 0.3, being smaller for elongated configurations and for large values of r_o/a, with a the minor radius of the plasma column. The parameter $\lambda_K(\omega)$, which is contributed by the alpha particles, is given by

$$\lambda_K(\omega) = -\frac{4\pi^2 i}{B_p^2(r_o)s_o\xi_o}\int_o^{r_o} drr^2 \int_{-\pi}^{\pi}\frac{d\theta}{2\pi}[\bar{e}_{||}\times\bar{\kappa}\cdot\nabla(\tilde{p}_{\perp\alpha}+\tilde{p}_{||\alpha})]\exp(i\omega t - iR) \quad (16)$$

to lowest order in ϵ_o. The parallel component of the pressure was neglected in the expression for $\lambda_K(\omega)$ given in Ref.[30] as the ordering $p_{||h} \sim \epsilon_o p_{\perp h}$ was assumed.

Following Eq.(10), the parameter $\lambda_K(\omega)$ is also split in two terms,

$$\lambda_K(\omega) = \lambda_K^{ad} + \lambda_K^{nad}(\omega), \quad (17)$$

where

$$\left.\begin{matrix}\lambda_K^{ad}\\ \lambda_K^{nad}(\omega)\end{matrix}\right\} = \frac{4\pi}{B_p^2(r_o)s_oR_o\xi_o}\int_o^{r_o} rdr\oint d\theta\left\{\begin{matrix}\hat{p}_\alpha^{ad}\cos\theta\\ \tfrac{1}{2}(\hat{p}_{||\alpha}+\hat{p}_{\perp\alpha})^{nad}\cos(q\theta)\end{matrix}\right. \quad (18)$$

with $\hat{p}_\alpha^{ad}$ and $(\hat{p}_{\perp\alpha}+\hat{p}_{||\alpha})^{nad}$ the corresponding moments of the adiabatic and non-adiabatic parts of $\hat{f}_\alpha$. Their explicit expression is given in the Appendix. Since $\hat{f}_\alpha^{ad}$ is independent of the pitch angle variable, the adiabatic pressure response is isotropic i.e. $\hat{p}_{\perp\alpha}^{ad} = \hat{p}_{||\alpha}^{ad} = \hat{p}_\alpha^{ad}$. It follows that $\hat{p}_\alpha^{ad}$ is independent of the poloidal angle to leading order in ϵ_o. Therefore

$$\lambda_K^{ad} = 0\ (\epsilon_o^2\ \beta_{p\alpha}). \tag{19}$$

By contrast, the non-adiabatic pressure response is mainly contributed by trapped alpha particles localised poloidally in the outer region of the plasma torus. Thus we find

$$\lambda_K^{nad} = 0\ (\epsilon_o^{3/2}\ \beta_{p\alpha}), \tag{20}$$

so that $\lambda_K(\omega) = \lambda_K^{nad}(\omega)[1 + 0(\epsilon_o^{1/2})]$, i.e. to lowest order the adiabatic part of the alpha particle pressure response can be neglected. More generally, this result holds for weakly anisotropic distributions such that $p_{\perp h} \sim p_{\|h}$, in which case both $p_{\perp h}$ and $p_{\|h}$ have a poloidal modulation of order ϵ_o [31]. This would be the case e.g. for the alpha particles produced in a spin polarised plasma with spins aligned along the magnetic field lines [32]. It is also worth noting that our expression for λ_K^{ad} corresponds to that derived by Mikhailovskii in Ref.[33]. In the latter paper, trapped particle effects, which lead to λ_K^{nad}, were neglected. Thermal trapped particle effects on internal kink modes were later included in Ref.[34] for frequencies in the range $\omega_D^{(o)} < \omega < \omega_b$.

To evaluate λ_K, we consider an isotropic slowing down distribution function,

$$F_{o\alpha} = \frac{3}{4\pi}\left(\frac{m_\alpha}{2}\right)^{3/2} \frac{p_\alpha/\epsilon_\alpha}{1 + 2\chi\epsilon_c/3\epsilon_\alpha} \frac{\theta(\epsilon_\alpha - \epsilon)}{\epsilon_c^{3/2} + \epsilon^{3/2}}, \tag{21}$$

where $p_\alpha = p_\alpha(r)$ is the equilibrium pressure of the alpha particles, ϵ_α = 3.5MeV is their birth energy, $\epsilon_c \sim (3\sqrt{\pi}/4)^{2/3}(m_\alpha/m_i)(m_i/m_e)^{1/3}T_e$ is the

critical energy at which the alpha particles transfer an equal amount of energy to the bulk ions and to the electrons via Coulomb collisions, $\chi = \ell n\,[(1 + \zeta_c)/(1 - \zeta_c + \zeta_c^2)^{1/2}] - \sqrt{3}\{(\pi/6) + \text{arctg}\,[(2 - \zeta_c)/(\sqrt{3}\zeta_c)]$, and $\zeta_c = (\epsilon_c/\epsilon_\alpha)^{1/2}$. By inserting (21) into (16) we obtain (see the Appendix for details)

$$\lambda_K(\omega) \simeq (\epsilon_o^{3/2}/s_o)\beta_{p\alpha}\,\Lambda_K(\omega/\bar{\omega}_{D\alpha}), \tag{22}$$

where $\bar{\omega}_{D\alpha} = \omega_{D\alpha}^{(o)}$ $(\epsilon = \epsilon_\alpha,\ \Lambda = 1 + \epsilon_o,\ r = r_o) = c\epsilon_\alpha/(2eBR_o r_o)$, and the natural definition of $\beta_{p\alpha}$, apart from corrections of order 1-q and s_o, is

$$\beta_{p\alpha} = \frac{-8\pi}{B_p^2(r_o)} \int_0^1 dx\, x^{3/2}\, \frac{dp_\alpha}{dx}\ , \tag{23}$$

where $x = r/r_o$. A more general expression of the coefficient $\beta_{p\alpha}$ is given in the Appendix, by Eq.(A.22). Peaked pressure profiles give comparatively larger values of $\beta_{p\alpha}$ (at constant total alpha particle energy content). For isotropic slowing down distributions the complex form factor Λ_K, whose explicit definition is given in the Appendix [Eq.(A.24)], depends on the q profile through $\omega_{D\alpha}^{(o)}$ [see Appendix], and only weakly on r_o/a, on $\epsilon_c/\epsilon_\alpha$ (for $\epsilon_c/\epsilon_\alpha \ll 1$) and on pressure profiles. For the sake of simplicity, these weak dependences will be neglected in the following numerical computations.

Graphs of Re Λ_K and Im Λ_K versus $\hat{\omega}_R$, where $\hat{\omega}_R \equiv$ Re $\hat{\omega}$, $\hat{\omega} \equiv \omega/\bar{\omega}_{D\alpha}$, are shown in Fig.1, displaying the standard features of a dispersion curve. A parabolic q profile inside the q = 1 surface has been assumed. The real part of Λ_K is negative and thus stabilising for $\hat{\omega}_R < \hat{\omega}_o \simeq 0.75$, i.e. for modes trailing the mean ∇B + magnetic curvature drift of the energetic ions. It is

positive, i.e. destabilising for modes that are leading, i.e. for $\hat{\omega}_R > \hat{\omega}_o$. For larger $\hat{\omega}_R$, Re $\lambda_K \propto \hat{\omega}_R^{-1} \epsilon_o^{3/2} \beta_{p\alpha}/s_o$. When $\hat{\omega}_R > \epsilon_o^{-1/2}$, Re λ_K becomes of higher order in ϵ_o and can be neglected when compared to the thermal plasma response. Im $\lambda_K/\bar{\omega}_{D\alpha}$ is negative for $\hat{\omega}_R > 0$ and $\beta_{p\alpha} > 0$. $\lambda_K(\omega)$ can be continued to negative values of ω_R, where Im λ_K becomes negligible, while Re λ_K goes monotonically to zero from negative values as $\hat{\omega} \to -\infty$. Negative values of $\hat{\omega}_R$ are of interest in the consideration of fast electron effects on internal m = 1 modes.

III DISPERSION RELATION, STABILITY DOMAIN, AND UNSTABLE REGIMES

In the transition layer near the q = 1 surface, the normal mode equation including the inertial term but neglecting resistive and other dissipative effects is [16]

$$\frac{d}{dz}\left\{\left[\frac{\omega(\omega - \omega_{di})}{\omega_A^2} - s_o^2 z^2\right]\frac{d\hat{\xi}_r}{dz}\right\} = 0 , \tag{24}$$

with $z = (r - r_o)/r_o$. Eq.(24) is valid provided the gyroradius of the thermal ions is smaller than the width of the transition layer, which is approximately given by $\delta \sim |\lambda_H + \lambda_K| r_o$. The modifications of the stability analysis in the large gyroradius limit are discussed in Section V.

Equation (24) is solved subject to the boundary conditions that, for $z/\delta > 1$, ensure the matching of the layer solution onto the outer solution given in Eq.(14). This leads to the radial displacement near the q = 1 surface,

$$\xi_r(x) = \frac{1}{2}\,\xi_o\left[1 - \frac{2}{\pi}\,\mathrm{arctg}\left(\frac{s_o z}{\lambda_H + \lambda_K}\right)\right], \tag{25}$$

and to the dispersion relation given in Eq.(2). Note that the eigenfunction (25) is regular for $\lambda_H + \mathrm{Re}\,\lambda_K \geq 0$.

A. Stable domain

On the basis of the dispersion relation (2), marginal stability is possible for $\omega_R \equiv \mathrm{Re}\,\omega > \omega_{di}$ when $\beta_{p\alpha} \neq 0$, and for $\omega_{di}/2 \leq \omega \leq \omega_{di}$ when $\beta_{p\alpha} = 0$. The marginal stability condition is obtained from the system

$$[\hat{\omega}_R(\hat{\omega}_R - \hat{\omega}_{di})]^{1/2} = -\,\hat{\beta}_{p\alpha}\Lambda_{KI}(\hat{\omega}_R) , \tag{26}$$

$$\hat{\gamma}_{mhd} + \hat{\beta}_{p\alpha}\Lambda_{KR}(\hat{\omega}_R) = 0 \ , \tag{27}$$

where we have defined $\hat{\omega}_{di} = \omega_{di}/\bar{\omega}_{D\alpha}$, $\Lambda_{KR} \equiv \text{Re}\ \Lambda_K$, $\Lambda_{KI} \equiv \text{Im}\ \Lambda_K$, Λ_K has been introduced below Eq.(23),

$$\hat{\gamma}_{mhd} \equiv \frac{\omega_A}{\bar{\omega}_{D\alpha}} \lambda_H = \frac{\gamma_{mhd}}{\bar{\omega}_{D\alpha}} \ , \tag{28}$$

and

$$\hat{\beta}_{p\alpha} \equiv \frac{\omega_A}{\bar{\omega}_{D\alpha}} \frac{\epsilon_o^{3/2}}{s_o} \beta_{p\alpha} \ . \tag{29}$$

The parameter $\hat{\beta}_{p\alpha}$ is proportional to the alpha particle density and depends on the alpha particle profiles, but is independent of their average energy. The resulting marginal stability curve in the $(\hat{\gamma}_{mhd}, \hat{\beta}_{p\alpha})$ plane is shown in Fig.2 for $\hat{\omega}_{di} = 0.05$. The corresponding values of the frequency at marginal stability are shown in Fig.3. Note that $\hat{\omega}_R$ increases smoothly with $\hat{\beta}_{p\alpha}$ from $\omega_R = \omega_{di}$ to $\omega_R \sim \bar{\omega}_{D\alpha}$. However, for $\hat{\omega}_{di} < 0.05$, a discontinuity of the frequency along the boundary of the stable domain occurs. In this case in a portion of the unstable domain, for a given pair of values of $\hat{\gamma}_{mhd}$ and $\hat{\beta}_{p\alpha}$, the higher frequency branch is unstable for two different values of the oscillation frequency as shown in Fig.4. A similar behaviour can also be found for different fast ion distribution functions resulting in a more abrupt change of $\Lambda_{KI}(\hat{\omega})$ around $\hat{\omega} = 1$.

The shape of the stability curve is determined by the mechanism discussed in Sec. I, which is such that the non-resonant response of the energetic alphas is stabilising at low frequency and destabilising at high frequency relative to the alpha particle magnetic drift frequency. It

follows that there exists a maximum value of $\gamma_{mhd}/\bar{\omega}_{D\alpha}$ above which stability is no longer possible. In addition, since the mode frequency increases with $\hat{\beta}_{p\alpha}$ along the marginal stability curve (Fig.3), the stable domain is also limited by a maximum $\hat{\beta}_{p\alpha}$.

The stable domain is weakly dependent on plasma parameters by virtue of the weak dependence of $\Lambda_K(\hat{\omega})$ on them, while the dependence on the q profile can be significant. Once $\Lambda_K(\hat{\omega})$ is given, the solution of Eqs.(26)-(27) depends on the parameter $\hat{\omega}_{di}$ only. Marginal stability curves for different values of $\hat{\omega}_{di}$ are shown in Fig.4. It can be seen that for $\hat{\omega}_{di} \gtrsim 0.05$, $\hat{\omega}_{di}$ has a destabilising effect in so far as the maximum stable value of $\hat{\gamma}_{mhd}$ is of interest. Again this can be understood by recalling that the frequency of this branch of the dispersion relation increases with $\hat{\omega}_{di}$ at low constant values of $\hat{\beta}_{p\alpha}$. However, larger values of $\hat{\beta}_{p\alpha}$ are needed to enter the stable domain from the left for decreasing $\hat{\omega}_{di}$ when $\hat{\omega}_{di} \lesssim \hat{\omega}_m$ (see Fig.4), with $\hat{\omega}_m \simeq 0.1$ the frequency at which Λ_{KR} is minimum. Similar conclusions can be drawn from the analysis of the stability curve in the $(\hat{\omega}_{di}, \hat{\beta}_{p\alpha})$ plane (Fig.5). Note in particular that there is a maximum value of $\hat{\omega}_{di}$ above which stability is no longer possible.

Eliminating $\hat{\beta}_{p\alpha}$ from Eqs.(26) and (27), one has

$$\hat{\gamma}_{mhd}(\hat{\omega}_R) = [\hat{\omega}_R(\hat{\omega}_R - \omega_{di})]^{1/2} \frac{\Lambda_{KR}(\hat{\omega}_R)}{\Lambda_{KI}(\hat{\omega}_R)} . \tag{30}$$

This expression shows that the maximum value, $\hat{\gamma}^{max}_{mhd}$, of $\hat{\gamma}_{mhd}(\hat{\omega}_R)$ depends on the phase of Λ_K and on $\hat{\omega}_{di}$. The maximum stable value of $\hat{\beta}_{p\alpha}$ is given by the formula

$$\hat{\beta}^{max}_{p\alpha} = - [\hat{\omega}_H(\hat{\omega}_H - \hat{\omega}_{di})]^{1/2}/\Lambda_{KI}(\hat{\omega}_H), \tag{31}$$

where $\hat{\omega}_H$ is the higher frequency solution of the equation $[\hat{\omega}_R(\hat{\omega}_R - \hat{\omega}_{di})]^{1/2}$ $[\Lambda_{KR}(\hat{\omega}_R)/\Lambda_{KI}(\hat{\omega}_R)] - \hat{\gamma}_{mhd} = 0$.

B. Resonant and fluid-like unstable regimes

Above the marginal stability curve, the higher frequency branch of the dispersion relation (2) is unstable. While the source of available energy to excite the mode is always measured by the parameter $\lambda_H + \mathrm{Re}\,\lambda_K$, the nature of the instability changes significantly in the different regimes. Just outside the stable domain, the mode has a frequency of oscillation $\hat{\omega}_R$ considerably larger than its growth rate $\hat{\gamma} \equiv \mathrm{Im}\,\omega/\omega_{D\alpha}$. Then, the dissipation provided by the resonance between the mode and energetic trapped ions plays an essential role. At small values of $\hat{\beta}_{p\alpha}$, it allows the source of excitation energy, which would otherwise be inaccessible due to the ω_{di}-stabilization, to be tapped. At large $\hat{\beta}_{p\alpha}$, it determines the mode frequency raising it to values such that Λ_{KR} turns positive. A consequence of the resonant interaction is the scattering of the energetic resonant ions. Therefore, these regimes appear as viable candidates to explain the initial linear rise of fishbone-like fluctuations. Further away from the stable domain, $\hat{\gamma} \gtrsim \hat{\omega}_R$ and the unstable mode is essentially an ideal MHD internal m = 1 mode with kinetic corrections arising from the fast ions and from the thermal ion finite diamagnetic frequency.

The lower corner region to the left of the stable domain in Fig.6, where $\omega_{di} > \gamma_{mhd} > \omega_A|\lambda_K|$, corresponds to the regime studied in Ref.[21], which is a natural extension to the case where $\omega_{di}/\omega_{Dh} \ll 1$ of the original fishbone model of Ref.[14]. The solution of the dispersion relation (2) in this domain can be obtained perturbatively by setting $\hat{\omega} = \hat{\omega}_{di} + \delta\hat{\omega}$. The mode growth rate

$$\hat{\gamma} = \mathrm{Im}\ \hat{\delta\omega} = 2\hat{\beta}_{p\alpha} \left| \frac{\Lambda_{KI}(\hat{\omega}_{di})}{\hat{\omega}_{di}} \right| [\hat{\gamma}_{mhd} - \hat{\beta}_{p\alpha} |\Lambda_{KR}(\hat{\omega}_{di})|] \qquad (32)$$

is determined by the resonant part of λ_K. The boundary of this region can thus be defined as the marginal stability condition when the resonant term is neglected in Eq.(2). This boundary, dashed in Fig.6, is obtained by imposing that the equation

$$[\hat{\omega}(\hat{\omega}_{di} - \hat{\omega})]^{1/2} = \hat{\gamma}_{mhd} + \hat{\beta}_{p\alpha}\Lambda_{KR}(\hat{\omega}) \qquad (33)$$

has coincident roots, which can occur for $\hat{\omega} < \hat{\omega}_{di}$. The dashed curve is interrupted for values of $\hat{\beta}_{p\alpha}$ such that $\hat{\beta}_{p\alpha}\Lambda_{KI} \sim \hat{\gamma}_{mhd} + \hat{\beta}_{p\alpha}\Lambda_{KR}$, for which it is no longer justified to treat the resonant term as a perturbation. Above the dashed curve the m=1 instability has a fluid-like character, as its growth rate is not determined by the resonant term.

For $\hat{\beta}_{p\alpha}$ exceeding the value corresponding to the peak of the stable domain in the $(\hat{\gamma}_{mhd}, \hat{\beta}_{p\alpha})$ plane, the dissipative part of λ_K is larger than the reactive part. Then, the nature of the instability changes completely. For $\hat{\omega} >> \hat{\omega}_{di}$ we obtain from Eq.(2)

$$\hat{\gamma} = \hat{\gamma}_{mhd} + \hat{\beta}_{p\alpha}\Lambda_{KR} \qquad (34)$$

$$\hat{\omega}_R = -\hat{\beta}_{p\alpha}\Lambda_{KI} \qquad (35)$$

The growth rate $\hat{\gamma}$ in Eq.(34) is given by the ideal MHD growth rate, $\hat{\gamma}_{mhd}$, modified by the reactive part of the alpha particle contribution, while the dissipative part determines the mode oscillation frequency. The effect of the resonance is to bring the mode frequency up to values of $\omega \lesssim \bar{\omega}_{D\alpha}$, where

Λ_{KR} changes sign and the energetic ions become destabilising. When $\hat{\gamma}_{mhd}$ is negligible, this high frequency mode is entirely supported by the energetic ion population for values of $\hat{\beta}_{p\alpha} > \hat{\beta}_{p\alpha}^{max}$, with $\hat{\beta}_{p\alpha}^{max}$ given in Eq.(31). In this limit, near marginal stability, $\hat{\omega} \approx \hat{\omega}_o$ and the growth rate is

$$\hat{\gamma} = \hat{\omega}_o \left(\frac{\partial \Lambda_{KR}}{\partial \hat{\omega}}\right)_{\hat{\omega}_o} (\hat{\beta}_{p\alpha} - \hat{\beta}_{p\alpha}^{max}), \qquad (36)$$

where we have used $\partial \Lambda_{KI}/\partial \hat{\omega} \simeq 0$ for $\hat{\omega} \sim \hat{\omega}_o$. This limit corresponds to the one analysed in Ref.[15]. A precise boundary between the high frequency resonant regime and the fluid-like regime cannot be defined, e.g. following the rule that we used on the left of the stable domain. However, the transition between the two regimes can be identified as the region where the solution of the dispersion relation is such that the reactive and the dissipative parts of the fast ion contribution are of the same order. This region is indicated in Fig.6 by a wiggled curve.

In Fig.7, the stable domain and unstable regimes are shown in the ($\hat{\omega}_{di}$, $\hat{\beta}_{p\alpha}$) plane at constant $\hat{\gamma}_{mhd}$. The region where the growth rate is essentially determined by $\hat{\gamma}_{mhd}$ is now confined to the lower right corner delimited by the dashed line. For values of $2\hat{\omega}_{di} \sim 1$, there are no longer two distinct resonantly unstable regimes. The region limited from below by the stable domain and by the dashed curve and, to the right, by $\hat{\omega}_{di} > \hat{\beta}_{p\alpha}$ corresponds to the domain of validity of the analysis in Ref.[14].

Examples of the numerical solution of the dispersion relation are shown in Fig.8, where the growth rate and oscillation frequency are plotted versus $\hat{\beta}_{p\alpha}$ for constant values of $\hat{\gamma}_{mhd}$ and $\hat{\omega}_{di}$. When $\hat{\beta}_{p\alpha} = 0$ and $\hat{\gamma}_{mhd} < \hat{\omega}_{di}/2$, the mode is purely oscillatory due to the stabilising effect of the thermal ion diamagnetic frequency. The growth rate initially increases with $\hat{\beta}_{p\alpha}$, reaches a maximum value approximately given by

$$\hat{\gamma}^{max} = C_o \hat{\gamma}^2_{mhd} \qquad (37)$$

before decreasing to zero at the left boundary of the stable domain. This behaviour is well represented by the analytic expression in Eq.(32). For the form factor Λ_K of Fig.1, $C_o = 1.2$. The mode is again destabilised for values of $\hat{\beta}_{p\alpha}$ such that the high frequency fishbone region to the right of the stable domain is entered. When $\hat{\gamma}_{mhd} > \hat{\omega}_{di}/2$, the ideal MHD internal (m = 1 mode) is unstable at $\hat{\beta}_{p\alpha} = 0$. The growth rate is reduced as $\hat{\beta}_{p\alpha}$ increases. The change in the slope of the curves on the right of Fig.8 corresponds to the crossing of the dashed line in Fig.6 and the entry in the fishbone domain with $\omega \sim \omega_{di} > \gamma$.

From the discussion in this section, it becomes clear why the existence of a stable domain was not foreseen by the original analyses of the fishbone instability in Refs.[14,15,21]. In Ref.[14], the limit $\omega_{di}/\bar{\omega}_{Dh} \sim 1$ was considered, in which case the stable domain disappears. However, when the analysis of Ref.[14] was extended to the case of isotropic alpha particles [21] and the case $\omega_{di}/\bar{\omega}_{D\alpha} << 1$ was considered, the approximation $|\lambda_K| < \lambda_H$, valid at low $\beta_{p\alpha}$, excluded the stable domain. The existence of a finite stability window did not appear in the analysis of Ref.[15] because of two simultaneous approximations: (i) $\omega_{di}/\bar{\omega}_{Dh} = 0$, and (ii) a simplified model of $\lambda_K(\omega)$ was used, yielding $\lambda_K = 0$ at $\omega = 0$. As a consequence of these two assumptions, the width of the stable domain shrinks to zero.

C. Stability of the resistive internal m = 1 branch

When $\lambda_H + Re\lambda_K$ is positive, a dissipative correction to the dispersion relation (2) arising from thermal particle collisions can be introduced perturbatively. Then, as stated in the Introduction, the lower frequency (resistive) branch of the dispersion relation can become unstable if

resistivity, arising from electron-ion collisions, overcomes the "viscous" terms associated with the ion-ion collisions and with the mode-energetic-ion resonance. However, when $\beta_{p\alpha}$ is sufficiently large, $\lambda_H + Re\lambda_K < 0$ and the stability of the lower frequency branch can no longer be described by Eq.(2). For this root we can approximate Re $\lambda_K(\omega) \approx$ Re $\lambda_K(0) < 0$. Then, as λ_H + Re $\lambda_K(0)$ becomes more negative with increasing $\beta_{p\alpha}$, a regime is entered where a proper description of the physics in the layer around the q = 1 surface has been shown [35-42] to lead to linear stability.

This point can be illustrated within the two-fluid description of the thermal plasma. Initially, we consider resistivity as the only dissipative process. The relevant dispersion relation, including the energetic ion effects according to the rule $\lambda_H \rightarrow \lambda_H + \lambda_K(\omega)$, is [14,16]

$$[\omega(\omega - \omega_{di})]^{1/2} = i\omega_A[\lambda_H + \lambda_K(\omega)] \frac{Q^{3/2}}{8} \frac{\Gamma[(Q-1)/4]}{\Gamma[(Q+5)/4]} , \qquad (38)$$

where

$$Q^2 = i\omega_A^{-3}\epsilon_\eta^{-1}\omega(\omega - \omega_{di})(\omega - \omega_{*e}) , \qquad (39)$$

with $\epsilon_\eta = \eta_{||}s_o^2c^2/(4\pi r_o^2\omega_A)$ the inverse magnetic Reynolds' number, $\eta_{||}$ the parallel resistivity, and $\omega_{*e} = (cT_e/eBr_on_e)[dn_e/dr + 1.71(n_e/T_e)dT_e/dr]_o$ the electron drift frequency at the q = 1 surface. For the sake of simplicity we set $\omega_{di} = -\omega_{*e}$. Equation (2) is recovered in the limit $|Q| >> 1$.

As shown in Refs.[35,36], a stable domain against both resistive and drift-tearing m = 1 modes exists for $\Omega_{di} \equiv |\omega_{di}/(\omega_A\epsilon_\eta^{1/3})| > 1$ and for $\Lambda_{HK} \equiv [\lambda_H + \lambda_K(0)]/\epsilon_\eta^{1/3}$ negative and such that $\Omega_{di}^{-1/2} < |\Lambda_{HK}| < \Omega_{di}$. In the drift tearing domain, characterised by the inequalities $|\Lambda_{HK}| > \Omega_{di} > |\Lambda_{HK}|^{-4/5}$ and $\Lambda_{HK} < 0$, modes are very weakly unstable or completely stable in the presence

of electron thermal conductivity [37,38]. Toroidal effects of the type described in Ref.[39] may also lead to complete stability of the m = 1 tearing mode when Ω_{di} is negligible, provided Λ_{HK} is negative and sufficiently large in absolute value.

In an ignition experiment, on account of the high plasma temperature, the parameter Ω_{di} is significantly larger than unity. Thus the relevant threshold is $\Lambda_{HK} < -\Omega_{di}^{-1/2}$. Expressing this threshold in terms of the alpha particle poloidal beta, we conclude that the resistive branch is suppressed by the energetic ions when

$$C \frac{\epsilon_o^{3/2}}{s_o} \beta_{p\alpha} \gtrsim \lambda_H + |\epsilon_\eta \omega_A/\omega_{di}|^{1/2}, \qquad (40)$$

where $C \approx |\Lambda_K(0)|$. For vanishing resistivity, this condition reduces to Eq.(4).

Stabilisation can occur for values of $\beta_{p\alpha}$ lower than indicated by Eq.(40) when ion dissipation processes are considered. As shown in Ref.[40], transverse (Braginskii's) viscosity arising from bulk ion-ion collisions is strongly stabilising when $|\Lambda_{HK}| < 1$ and Ω_{di} is large. An even stronger ion collisional damping can be expected in the neoclassical banana regime [41,42]. We recall that, when $|\Lambda_{HK}|$ is small, the resistive m = 1 mode is nearly purely growing in the plasma rest frame, so that the contribution of the mode-fast ion resonance is negligible. The latter becomes more important than collisional viscosity when $\Lambda_{HK} > 1$, as the m = 1 mode acquires a frequency of oscillation $\omega_R \lesssim \omega_{di}/2$. In this regime, the stability threshold of the lower frequency branch is determined by the balance between resistivity and the resonant term [13].

A numerical example of the lower frequency solution of the relevant

dispersion relation at $\lambda_H = 0$, including resistivity and a small bulk ion viscosity [40], is shown in Fig.9. The parameters are chosen so that when $\beta_{p\alpha} = 0$, a positive growth rate is found. The instability is suppressed for values of $\beta_{p\alpha}$ in agreement with the threshold given above.

The above results are intended to be indicative since, as noted in Ref.[13], the two fluid model is not entirely appropriate in low collisionality regimes, which are approached, e.g. in JET during sawtooth free periods, and which are relevant to an ignited plasma. In these regimes, the resistive instability can be expected to be even weaker.

In Refs.[26], a model for λ_K such that $\lambda_K(0) = 0$ was used. Then the basic stabilisation mechanism that we have described, which consists in pushing $\lambda_H + \mathrm{Re}\ \lambda_K$ to negative values by increasing $\beta_{p\alpha}$, cannot be realised. Within such a model, the only possibility to obtain full stabilisation is to keep λ_H positive and sufficiently large. In this case, as we have already noted, the mode acquires a finite frequency of oscillation related to ω_{di}, and conditions can be found where the mode-particle resonance prevails over resistivity. Consequently, in the second of Refs.[26], the conclusion was reached that only for values of β_p in excess of the ideal MHD stability threshold $\beta_{p,mhd}$ by an amount determined by resistivity could the $m = 1$ instability be completely suppressed in the presence of energetic ions. In contrast, we have shown that, if a model for $\lambda_K(\omega)$ which properly reproduces the zero-frequency energetic ion response is used, the condition $\beta_p > \beta_{p,mhd}$ for fast ion stabilisation is not required.

IV SCALING OF THE STABILITY THRESHOLDS

We are now in the position to quantify the scaling of the stability thresholds in terms of the plasma parameters [43]. In order to obtain expedient estimates, we adopt a simplified model for the ideal MHD energy functional:

$$-\delta W_{min} \propto \lambda_H \approx \frac{3\pi}{2} \epsilon_o^2 \, (\beta_p^2 - \beta_{p,mhd}^2). \tag{41}$$

This model has been initially derived [18] for a toroidal plasma with circular cross section, in the limit where the q profile in the region where $q \leq 1$ can be approximated by a parabola, and $1-q_o$ is relatively small. The same model can also be used for non circular plasmas, provided the ideal MHD threshold $\beta_{p,mhd}$ is appropriately modified [19]. The relevant definition of the poloidal beta parameter β_p is given by Eq.(15), together with the typical range of variation of $\beta_{p,mhd}$ for varying q = 1 radii and plasma shaping.

The maximum stable values of β_p and $\beta_{p\alpha}$ in the presence of alpha particles is obtained from Eqs.(28)-(31), and (41). As an example, for the realistic value $\hat{\omega}_{di} = 0.05$, and for the form factor Λ_K in Fig.1,

$$(\beta_p^{max})^2 = \beta_{p,mhd}^2 + 7.8 \times 10^{-2} \, \frac{\bar{\omega}_{D\alpha}}{\omega_A} \left(\frac{R_o}{r_o}\right)^2 \tag{42}$$

and

$$\beta_{p\alpha}^{max} = 0.45 \, s_o \, \frac{\bar{\omega}_{D\alpha}}{\omega_A} \left(\frac{R_o}{r_o}\right)^{3/2}. \tag{43}$$

In Eq.(43) we have chosen $\beta_p = \beta_{p,mhd}$. Expressing the ratio $\bar{\omega}_{D\alpha}/\omega_A$ in terms

of $n_i(r_o)$, B, r_o, R_o and neglecting terms of order $(\beta_{p,mhd}/\beta_p^{max})^2$ Eq.(42) reduces to Eq.(5). Similarly,

$$\beta_{p\alpha}^{max} = 1.2 \frac{(n_{io}/10^{15}cm^{-3})^{1/2}(2s_o)}{(6r_o/R_o)^{5/2}(R_o/1.2m)(B/10^5G)} , \qquad (44)$$

Using Eqs.(28), (29), and (42), we can represent the stability domain in the plane $(\Delta\beta_p^2 - \beta_{p\alpha})$, where $\Delta\beta_p^2 \equiv \beta_p^2 - \beta_{p,mhd}^2$, once the values of ϵ_o, s_o, $\bar{\omega}_{D\alpha}/\omega_A$, and ω_{di}/ω_A are given. In this plane, the width and the height of the stable domain scale as strong inverse powers of the q=1 radius. In fact, from Eqs.(43) and (44), neglecting the weak radial dependence of the density, one finds approximately $\beta_p^{max} \propto r_o^{-3/2}$ and $\beta_{p\alpha}^{max} \propto r_o^{-5/2}$. Therefore, it becomes increasingly difficult to suppress the m = 1 mode as the q = 1 radius expands. This is shown in Fig.10. Three examples are given, corresponding to three values of r_o/a at fixed a/R_o, s_o, and plasma profiles. We have taken $n_i = n_i(0)(1-r^2/a^2)^{\sigma_n}$ and $T_i = T_i(0)(1-r^2/a^2)^{\sigma_T}$ with $\sigma_n = 1$, $\sigma_T = 3/2$, which gives $\bar{\omega}_{D\alpha}/\omega_A \propto (a/r_o)(1-r_o^2/a^2)^{1/2}$ and $\omega_{di}/\bar{\omega}_{D\alpha} \propto (r_o/a)(1-r_o^2/a^2)^{1/2}$. The q profile was chosen to be $q(r) = q_o + (1 - q_o)(r/r_o)^2$ for $0 \le r \le r_o$, with $q_o = 0.8$ for all three cases.

In an ignited plasma $\beta_{p\alpha}$ and β_p are not independent parameters. Following Ref.[44] we recall that the alpha particle pressure scales as $p_\alpha \sim T_e^{3/2} n_i \langle\sigma_F v\rangle$, where the reaction rate $\langle\sigma_F v\rangle$ depends on the ion temperature. Then, the ratio p_α/p depends only on the bulk plasma temperature. For example, for $T_e = T_i = 20$ keV, one finds $p_\alpha/p \simeq 0.26$. The pressure profile of the alpha particles is thus obtained from the temperature and density profiles of the thermal plasma. Assuming parabola-like profiles as defined above, and $T_e = T_i$, p_α can be written as

$$p_\alpha(r) = p_\alpha(0)(1-r^2/a^2)^\sigma, \tag{45}$$

where, taking for simplicity $\langle\sigma_F v\rangle \propto T_i^2$ for $T_i \lesssim 25$ keV, we have $\sigma \leq (7\sigma_T/2) + \sigma_n$. The equality sign corresponds to the profile at birth. The diffusion from the location at birth due to the finite size of the particle orbit can be accounted for by considering a smaller value of σ, while keeping the alpha particle energy content constant.

By combining Eqs.(15), (23) and (45) we obtain

$$\frac{\beta_{p\alpha}}{\beta_p} = \frac{p_\alpha(0)}{p_o(0)}\, P(x_o,\sigma_n,\sigma_T,\sigma), \tag{46}$$

where the profile factor P is defined by

$$P = \frac{\sigma(\sigma+1)}{(\sigma_n+\sigma_T)(7\sigma_T/2 + \sigma_n+1)} \; \frac{\int_o^{x_o} dx\, x^{5/2}\,(1-x^2)^{\sigma-1}}{\int_o^{x_o} dx\, x^3\,(1-x^2)^{\sigma_n+\sigma_T-1}}, \tag{47}$$

with $x_o = r_o/a$. Plots of $\beta_{p\alpha}/\beta_p$ versus x_o for various central plasma temperatures are shown in Fig.11 for $\sigma_n = 1$, $\sigma_T = 3/2$, and $\sigma = 6$.

Equation (46) can be used to restrict the accessible portion of the $(\beta_p,\beta_{p\alpha})$ stability plane, once the central plasma temperature T(0) is given. Two examples are shown in Figs.12 and 13 for $r_a/a = 0.3$. and for $r_o/a = 0.5$, respectively, assuming $\beta_{p,mhd} = 0.2$ for both cases. A straight line corresponds to a fixed ratio $\beta_{p\alpha}/\beta_p$, as determined by Eq.(46). As the temperature increases, the slope of the straight line decreases and regions to the right of the stable domain become accessible. These examples indicate that the largest stable values of β_p can be attained at relatively low

ignition temperatures (T(0) $\sim$ 20 keV) and small values of r_o/a. The low frequency fishbone region to the left of the stable domain can always be visited if the ignition conditions are approached for values of $\beta_p \gtrsim \beta_{p,mhd}$. On the other hand, the more dangerous higher frequency fishbone regime with $\omega \sim \bar{\omega}_{D\alpha}$ can only be entered at relatively high values of T(0) and large r_o/a.

V LARGE THERMAL ION GYRORADIUS REGIME

Kinetic modifications of the dispersion relation (2) due to the thermal ions become important when their mean gyroradius, $\rho_i = (T_i/m_i)^{1/2}(m_i c/eB)$, is of the order of or larger than the width of the fluid transition layer at the $q = 1$ surface. In Ref.[28] it was shown that these effects lead to growth rates in the linear phase that are larger than those which would be obtained in the fluid approximation. The relevance of this kinetic regime to the analysis of fishbone excitation and sawtooth suppression has been pointed out recently [27].

A dispersion relation valid for arbitrary values of the ion gyroradius and negligible resistivity is given in Eq.(13) of Ref.[28]. Including the energetic particles according to the rule $\lambda_H \to \lambda_H + \lambda_K(\omega)$, this dispersion relation becomes

$$[\hat{\omega}(\hat{\omega}-\hat{\omega}_{di})]^{1/2}F(\nu) = i[\hat{\gamma}_{mhd} + \hat{\beta}_{p\alpha}\Lambda_K(\hat{\omega})] \ , \tag{48}$$

where

$$F(\nu) = 4\,\frac{(2\nu-1)^{1/2}}{(2\nu+1)^{3/2}}\,\frac{\Gamma^2(\frac{5+2\nu}{4})}{\Gamma^2(\frac{3+2\nu}{4})} \ , \tag{49}$$

$$\nu^2 = \frac{1}{4} - \frac{(\hat{\omega}+\tau\hat{\omega}_{*i})(\hat{\omega}-\hat{\omega}_{di})}{\hat{\rho}_i^2} \tag{50}$$

with $\tau = T_e/T_i$, $\hat{\omega}_{*i} = -(cT_i/eBr_o\bar{\omega}_{D\alpha})(d\ell nn_i/dr)$, and

$$\hat{\rho}_i = \frac{\sqrt{1+\tau}\,\rho_i}{r_o}\,\frac{s_o \omega_A}{\bar{\omega}_{D\alpha}}\,, \tag{51}$$

all parameters being evaluated at the q=1 surface. The fluid limit is recovered for $\hat{\rho}_i \ll 1$ ($|\nu| \gg 1/2$), where $F(\nu)$ approaches unity. The dispersion relation given in Eq.(13) of Ref.[28] has been derived for $\eta_i \equiv d\ell nT_i/d\ell nn_i = 0$. However it can be shown that for the higher frequency branch under consideration in this paper, it may be extended to $\eta_i \neq 0$ by re-defining the ion diamagnetic frequency $\hat{\omega}_{di}$ as $\hat{\omega}_{di} = \hat{\omega}_{*i}[1 + \alpha(\nu)\eta_i]$ where the real coefficient $\alpha(\nu)$ approaches unity in the fluid limit, and decreases to $\alpha(\nu) \simeq 0.5$ in the kinetic limit where $|\nu - 1/2| < 1$. For the sake of simplicity, we take $\alpha(\nu) \simeq$ const, which allows us to consider $\hat{\omega}_{di}$ as an independent parameter. We also consider equal electron and ion temperatures ($\tau=1$).

We are interested in the marginal stability condition arising from (50). For real frequencies, ν^2 acquires negative and positive real values. The mode eigenfunction becomes singular when $\nu^2 \leq 1/4$. However, this singularity is resolved [28] by a small resistivity, provided the determination of $(2\nu-1)^{1/2}$ is chosen corresponding to the branch-cut $-\infty < \mathrm{Re}\ \nu \leq 1/2$ and to $\nu = -i|\nu|\,\mathrm{sgn}(\omega_{di})$ for $\nu^2 < 0$, with $\mathrm{sgn}(x) = \pm 1$ for $x \gtrless 0$, respectively.

A plot of F versus real ν^2 is shown in Fig.14. F is complex for $\nu^2 < 0$, it is purely imaginary for $0 \leq \nu^2 < 1/4$, and it is real for $\nu^2 \geq 1/4$. When $\beta_{p\alpha} = 0$, the higher frequency branch of Eq.(48) is marginally stable if $\max[(\hat{\omega}_{di}/2),\ C_1\bar{\beta}\hat{\rho}_i] > \hat{\gamma}_{mhd} > \hat{\gamma}^{min}_{mhd}$, with

$$\hat{\gamma}^{min}_{mhd} = -\,|F(0)|\,[\hat{\omega}_\rho(\hat{\omega}_\rho - \hat{\omega}_{di})]^{1/2} \simeq -\,f(\bar{\beta})\hat{\rho}_i\,, \tag{52}$$

$C_1 \sim 1/3$, $|F(0)| \simeq 2.2$, $\hat{\omega}_\rho \equiv (\hat{\omega}_{di}^2 + \hat{\rho}_i^2/4)^{1/2}$, $\bar{\beta}_i = 4\omega_{di}^2/3\rho_i^2 = (L_s^2/r_p^2)\,\beta_{io}$, $\beta_{io} \equiv 8\pi p_i(r_o)/B^2$, $L_s \equiv R_o/s_o$, $r_p \equiv |d\ell n p_i/dr|^{-1}$, and $f(\bar{\beta})$ a numerical factor which varies monotonically between $f \simeq 0.77$ for $\bar{\beta} \gg 1$ and $f = 1.1$ for $\bar{\beta} \ll 1$. The mode frequency ranges in the interval $\hat{\omega}_{di}/2 < \hat{\omega}_R < \hat{\omega}_\rho$. This neutral mode is destabilised by the resonance with the energetic ions. Then, when $\beta_{p\alpha} \neq 0$, it becomes possible to excite fishbone oscillations for values of β_p below the MHD stability threshold $\beta_{p,mhd}$ [29], extending the instability domain obtained by the fluid thermal ion approximation [14]. The frequency in this extended domain is $\hat{\omega} = \hat{\omega}_{di}$ for $\bar{\beta} > 1$, and $\hat{\omega} = \hat{\rho}_i/2$ for $\bar{\beta} < 1$. This resonant mode does not rely on a finite thermal ion diamagnetic frequency, in contrast with the fluid instability condition in the fluid limit.

Examples of the marginal stability curve are shown in Figs.15 and 16. The frequency along the marginal stability curve increases with $\hat{\beta}_{p\alpha}$ from $\hat{\omega} = \hat{\omega}_\rho$ to $\hat{\omega} \sim 1$. In Fig.15 we have set $\hat{\omega}_{di} = 0$, in order to emphasise the existence of a fishbone regime to the left of the stable domain with a frequency not determined by either ω_{di} or $\bar{\omega}_{D\alpha}$. Figure 16 shows stability curves for $\hat{\omega}_{di} = 0.05$ and different values of $\hat{\rho}_i$. When $\hat{\rho}_i \ll 1$, the left boundary of the stable domain, which in the fluid bulk limit is approximately given by Eq.(4), is now shifted to the right by an amount $\delta\hat{\beta}_{p\alpha} \sim \hat{\gamma}_{mhd}^{min}$, i.e.

$$\delta\beta_{p\alpha} \sim (s_o/\epsilon_o^{3/2})(\rho_i/r_o), \tag{53}$$

while the right boundary of the stability curve is not significantly affected. For $\hat{\rho}_i \gtrsim 0.5$, the mode frequency becomes comparable or larger than the frequency $\hat{\omega}_o$ at which $\mathrm{Re}\,\lambda_K$ changes sign and the stable domain

disappears. Such high values of $\hat{\rho}_i$ are however unlikely to occur in the presently envisaged ignition experiments.

Resistive effects are important in the frequency range $\omega \sim \omega_\rho$ where they partly modify the stability boundary. These effects will be discussed in a separate paper.

VI CONCLUSIONS

We have shown that particles with energies in the MeV range in a magnetically confined, axisymmetric toroidal plasma can significantly affect the stability of m = 1, n = 1 internal modes. These particles modify both the reactive and the dissipative part of the plasma response and can cause either fishbone-like instabilities, or, under certain conditions, they can allow for stable values of the bulk plasma poloidal beta, β_p, significantly higher than those predicted by the ideal MHD theory. The stabilisation arises because energetic particles with poloidally trapped orbits experience a magnetic drift motion which on average is much faster than the characteristic phase velocity of m = 1 modes driven by the thermal plasma pressure gradient. Under these circumstances, energy must be spent to displace the fast particles, leading to a more favourable stability threshold, as given e.g. by Eq.(4) in the limit $\omega << \bar{\omega}_{Dh}$ (ω is the mode frequency in the plasma rest frame). If γ_{mhd} is the growth rate in the ideal MHD limit, then there is a maximum ratio of $\gamma_{mhd}/\bar{\omega}_{Dh}$ that can be stabilised, as shown in Fig.2. Since γ_{mhd} is related to β_p, this in turn implies a maximum stable value of β_p, estimated in Eq.(5) for the case of alpha particles produced in a DT burning plasma.

The focus of this paper has been on the effects of alpha particles produced isotropically in an ignition experiment. A number of theoretical issues have been addressed. Firstly, we have shown that the alpha particle response to the m = 1 perturbation, which is a function of $\omega/\bar{\omega}_{D\alpha}$, remains finite in the limit $(\omega/\bar{\omega}_{D\alpha}) \to 0$. As a consequence, it is possible to suppress overstable as well as purely growing modes. Since at low values of $\beta_{p\alpha}$ the mode frequency is related to the thermal ion diamagnetic frequency, ω_{di}, stabilisation can be demonstrated with the simplest ideal MHD model for

the plasma bulk where ω_{di} is set equal to zero. When resistive effects are considered, the use of the relevant dispersion relation shows that the energetic alpha particles can suppress the resistive m = 1 internal instability as well. Finite values of ω_{di} reduce the maximum stable β_p. In fact, as the value of ω increases with ω_{di} at constant $\beta_{p\alpha}$, the stabilisation mechanism becomes less effective (see Fig.4).

Secondly, we have clarified the relationship between the two models [14,15] of fishbone oscillations that have appeared in the literature. We have shown that, in the limit $\omega_{di}/\bar{\omega}_{D\alpha} \ll 1$, two distinct regimes exist where the m = 1 mode is destabilised by the resonant interaction with the trapped alpha particles (see Fig.6). In the first regime, corresponding to the analysis of Ref.[14] (see also Ref.[21]), $\beta_{p\alpha}$ is relatively low and the relevant mode frequency is related to ω_{di}. This mode is suppressed as $\beta_{p\alpha}$ is raised beyond the value indicated in Eq.(4) and the stable domain is entered. When $\beta_{p\alpha}$ exceeds a second threshold, given e.g. in Eq.(44) for λ_H negligible, the higher frequency branch of the dispersion relation (2) has $\omega \sim \bar{\omega}_{D\alpha}$. Since the reactive part of the alpha particle response changes sign for $\omega \sim \bar{\omega}_{D\alpha}$, an instability entirely supported by these particles becomes possible. This instability corresponds to the one analysed in Ref.[15]. We have shown that the higher frequency branch of the dispersion relation can be followed from one regime to the other along the marginal stability curve, where the oscillation frequency is found to increase from $\omega = \omega_{di}$ at low $\beta_{p\alpha}$ to $\omega \sim \bar{\omega}_{D\alpha}$ at large $\beta_{p\alpha}$ (see Fig.3). For intermediate values of $\beta_{p\alpha}$ and sufficiently large values of λ_H, a transition region exists where the fishbone instability has hybrid features, i.e. it is driven by the bulk plasma pressure gradient but has a frequency intermediate between ω_{di} and $\bar{\omega}_{D\alpha}$. For values of $\omega_{di} \sim \bar{\omega}_{D\alpha}$, there are no longer two distinct fishbone regimes.

Thirdly, we have extended these results to the large thermal ion gyroradius regime, along the lines of Ref.[28]. In this regime, the m = 1 instability in the linear phase is generally stronger than what would be predicted if the fluid approximation were used. The stable domain disappears when $\hat{\rho}_i \equiv \sqrt{1+\tau}\ (\rho_i/r_o)(s_o\omega_A/\bar{\omega}_{D\alpha}) \gtrsim 0.5$. For smaller values of $\hat{\rho}_i$, a stable domain persists, but in the $(\hat{\gamma}_{mhd}, \hat{\beta}_{p\alpha})$ plane (Fig.16) is eroded from the left by an amount $\delta\hat{\beta}_{p\alpha} \sim \hat{\rho}_i$. This eroded region is now occupied by fishbone oscillations with a frequency approximately determined by the maximum between ω_{di} and $(\rho_i/2r_o)\omega_A$. A novel result is that these fishbone oscillations occur in a wider parameter domain than that obtained in the fluid limit in Ref.[14] extending for vanishing resistivity to negative values of λ_H. This unstable regime extends that obtained in the fluid limit in Ref.[14].

Although this paper has mainly addressed the effects of isotropic fusion reaction products, most results apply equally well to a population of energetic ions distributed anisotropically in velocity space. Indeed, this theory was initially aimed [25,13] at explaining sawtooth suppression in JET discharges with high power ICRF heating [8]. In these discharges, minority ions are accelerated to mean energies $\epsilon_h \sim 1$ MeV, and can reach a pressure that is a substantial fraction of the total plasma pressure. In addition, the distribution of energetic ions is strongly anisotropic, with ratios of $p_{\perp h}/p_{\parallel h}$ believed to reach values of the order of ten or larger. When applying the present theory to the anisotropic case, it must be observed that, independently of the velocity space distribution, the order of magnitude of their contribution to the dispersion relation is related to the pressure of the poloidally trapped energetic fast ions. The second difference is that, when $p_{\parallel h} \lesssim (r_o/R_o)\ p_{\perp h}$, the zero frequency kinetic response vanishes with the average of 1-q within the q = 1 volume. Then, if $\langle 1-q \rangle$ is smaller than $\omega_{di}/\bar{\omega}_{Dh}$, the low-$\beta_{p\alpha}$ stability threshold

(corresponding to Eq.(4) for the $p_{\|h} \sim p_{\perp h}$ case) becomes $\lambda_H \sim s_o^{-1}\epsilon_o^{3/2}\beta_{ph}$ $[\omega_{di}/\bar{\omega}_{Dh} + O(\langle 1-q \rangle)]$, as shown in Refs.[13] and [20]. In addition, the actual fast ion distribution determines the detailed form of $\Lambda_K(\omega/\bar{\omega}_{Dh})$, from which the numerical factors in the relevant scalings are obtained.

Taking into account these differences arising from their large anisotropy, the energetic ions in JET ICRF heated plasmas can provide first-hand experimental information of the would-be alpha particle effects on m = 1 modes in an ignited plasma [45]. At moderate currents ($I_p \lesssim 3$ MA), sawteeth in JET can be suppressed in a reproducible manner for periods exceeding 3s and auxiliary powers $P_{RF} \gtrsim 4$ MW. In this case, values of $\beta_p \gtrsim 0.3$, i.e. in excess of the ideal MHD threshold, are often achieved, while $\omega_{di}/\bar{\omega}_{Dh} \sim 10^{-1}$. Experimental evidence in support of an active role of the energetic ions in suppressing the sawteeth was reported in Refs.[8] and [46]. Our predictions in Refs.[13] and [20] were found to be in reasonable agreement with the relevant experimental conditions. In this paper, we have shown that the stable domain shrinks considerably as the q = 1 radius is increased (see Fig.10). This, together with the fact that $\beta_{p,mhd}$ is usually lower at large r_o [18], may account for the increasing difficulty in stabilising sawteeth in JET for plasma currents $I_p > 3$ MA, as r_o tends to increase with I_p.

Fishbone-like oscillations have also been observed in JET during ICRF heating [12]. These oscillations have a low amplitude compared with that of the original PDX fishbones [9]. No noticeable loss of fast ions associated with the bursts is observed in JET, at least within the time resolution of the relevant diagnostics. Although more analysis is needed, the mode frequency in the initial rise of the burst appears to be correlated with the ion diamagnetic frequency. The weakness of these fluctuations, and the lack of significant fast ion losses may be explained by the fact that only those

minority ions that have slowed down to energies of the order of 100 keV can satisfy the relevant resonance condition.

These results indicate that fusion alpha particles can indeed help to control the onset of m = 1 internal modes in an ignited plasma. This control is most effective when the plasma region where q < 1 is not too large, while it becomes very difficult to suppress the m = 1 mode when $\beta_p > \beta_{p,mhd}$ and $r_o/a \gtrsim 0.5$. Other key parameters are $\bar{\omega}_{D\alpha}/\omega_A$ (to which both β_p^{max} and $\beta_{p\alpha}^{max}$ are proportional) and the central ignition temperature, T(0). The latter parameter determines the ratio $\beta_{p\alpha}/\beta_p$. It turns out that there exists an optimum value of T(0), typically T(0) = 20 keV, at which the largest stable values of β_p can be obtained (see Figs.12 and 13). If ignition is to be achieved at higher values of T(0), the enhanced stability is partly lost and, if also $r_o/a \gtrsim 0.5$, it becomes possible to excite high frequency fishbone oscillations with $\omega \sim \bar{\omega}_{D\alpha}$. The consequences of this instability can be rather unfavourable on the ignition energy balance, as newly born alpha particles carrying energies above 1 MeV would be scattered. However, under certain circumstances, this instability could have the desirable effect of preventing the thermonuclear runaway.

Kinetic effects of the thermal ions are expected to be important in ignition regimes. For a DT thermonuclear plasma, the relevant parameter can be rewritten as $\hat{\rho}_i = 0.4(T_{io}/3.5\ MeV)s_o\beta_{io}^{-1/2}$, where $\beta_{io} = 8\pi n_{io}T_{io}/B^2$, n_{io} and T_{io} are the thermal ion density and temperature at the q = 1 surface, and we have assumed $T_e \approx T_i$. Realistic values are $\hat{\rho}_i \sim 0.1$. For these values of $\hat{\rho}_i$, the main effect is an extension of the low frequency fishbone regime to negative values of λ_H and larger values of $\beta_{p\alpha}$ at the expense of the stable domain, as discussed previously in this section (see also Section V). This unstable regime could be entered at the onset of ignition, when $\beta_{p\alpha}$ is still

small. However, the instability should scatter slowed down alpha particles and is not expected to affect the energy balance significantly. In fact, it may even be beneficial in easing the problem of ash accumulation [21].

In conclusion, in order to avoid dangerous m = 1 instabilities in a fusion burning plasma, it is most favourable to operate at relatively low temperatures and small q = 1 radii, finding a compromise between minimising β_p and maximising $\bar{\omega}_{D\alpha}/\omega_A \propto n_{io}^{1/2}/(r_o B^2)$. An effective strategy would be to approach ignition conditions with the highest plasma currents, trying to keep β_p below its ideal MHD threshold. The current could be reduced after a substantial population of alpha particles has been produced, in order to diminish the q < 1 volume and increase the ratio $\bar{\omega}_{D\alpha}/\omega_A$. The stabilising influence of the fusion products on global plasma modes will then allow to raise β_p above its ideal MHD threshold.

ACKNOWLEDGEMENTS

The role played by R.J. Hastie in the early analysis of the sawtooth suppression mechanism and in pointing out the importance of the zero frequency response is gratefully acknowledged. We also thank H.L. Berk, D.J. Campbell, P. Detragiache, D.F. Düchs, T. Stringer, J.A. Wesson and Y.Z. Zhang for useful discussions. This work was sponsored in part by the U.S. Department of Energy.

APPENDIX - EVALUATION OF λ_K

In this Appendix we provide the main analytic steps in the evaluation of $\lambda_K(\omega)$. We start from the linearised Vlasov equation for the α-particles (we drop the subscript "α" to simplify the notation):

$$\frac{\partial \tilde{f}}{\partial t} + \bar{v}\cdot\nabla\tilde{f} - \Omega \frac{\partial \tilde{f}}{\partial \phi} = - \frac{2e}{m} (\tilde{\bar{E}} + \frac{1}{c} \bar{v} \times \tilde{\bar{B}})\cdot\nabla_v F_o, \tag{A.1}$$

where $F_o = F_o(r,\epsilon)$ is the equilibrium distribution function, $\Omega = 2eB/mc$ and ϕ is the gyroangle in velocity space. We seek a solution of Eq.(A.1) to leading order in the smallness parameters $\epsilon_o = r_o/R_o$ and $\epsilon_\rho = \rho/R_o$, with ρ the alpha gyroradius. This solution can be split in two parts [30], $\tilde{f} = \tilde{f}^{ad} + \tilde{f}^{nad}$, where

$$\tilde{f}^{ad} = - \bar{\xi}_\perp \cdot \nabla F_o, \tag{A.2}$$

$$\tilde{f}^{nad} = \epsilon \frac{\partial F_o}{\partial \epsilon} (1 - \frac{\omega_*^T}{\omega}) \tilde{h}, \tag{A.3}$$

where $\tilde{h}$ satisfies the equation

$$(\omega + i\bar{v}_D\cdot\nabla + iv_{||} \bar{e}_{||}\cdot\nabla)\tilde{h} = - \omega(\bar{\xi}_\perp \cdot \bar{\kappa}) \tag{A.4}$$

We have used $\tilde{\bar{E}} = (i\omega/c)\ \bar{\xi} \times \bar{B}$ and Eq. (8) to relate $\tilde{\bar{E}}$ and $\tilde{\bar{B}}$ to the plasma displacement vector $\bar{\xi}$ in Eqs.(A.2) and (A.4); ω_*^T is defined below Eq.(12), the magnetic drift velocity $\bar{v}_D$ is given in Eq.(13) and the subscripts $||$ and $\perp$ refer to the parallel and perpendicular directions to the equilibrium magnetic field, respectively.

We consider modes with frequencies $\omega < \omega_b$, ($<q-1>\omega_t$), with ω_b and ω_t the bounce and the transit frequencies of the trapped and circulating alpha particles. Then, the contribution of the circulating alphas to the solution of Eq.(A.4) can be neglected. To evaluate the trapped particle contribution, we expand $\tilde{h}$ in powers of (ω/ω_b). To lowest order, neglecting finite banana orbit effects, we have $\bar{e}_{||}\cdot\nabla \tilde{h}_o = 0$ This implies that $\tilde{h}_o$ must have the form

$$\tilde{h}_o = \hat{h}_o(r)\ e^{-i\omega t + iS} \ . \tag{A.5}$$

where $S = (\zeta - q\theta)$, such that $\bar{e}_{||}\cdot\nabla S = 0$ to leading order in ϵ_o. To next order in ω/ω_b, we have

$$(\omega + i\bar{v}_D\cdot\nabla)\ \tilde{h}_o + iv_{||}\ \bar{e}_{||}\cdot\nabla\tilde{h}_1 = -\ \omega(\bar{\xi}_{\perp}\cdot\bar{\kappa}) \tag{A.6}$$

Setting $\tilde{h}_1 = \hat{h}_1(r,\ \theta)\ \exp(-\ i\omega t + iS)$, and multiplying Eq.(A.6) by $\exp(i\omega t - iS)$, we obtain

$$(\omega - \bar{v}_D\cdot\nabla S)\ \hat{h}_o + iv_{Dr}\ \frac{d\hat{h}_o}{dr} + iv_{||}\ \frac{B_\theta}{Br}\ \frac{\partial}{\partial\theta}\ \hat{h}_1 = -\ \omega(\hat{\bar{\xi}}_{\perp}\cdot\bar{\kappa})\ \exp[i(R - S)] \tag{A.7}$$

where R is defined in Eq.(9).

Averaging along the particle orbits, the term involving v_{Dr}, which is odd in θ, and the term involving h_1 are annihilated. Thus we obtain

$$\hat{h}_o = -\ \frac{\omega}{\omega - \omega_D^{(o)}}\ \{(\hat{\bar{\xi}}_{\perp}\cdot\bar{\kappa})\ \exp[i(q - 1)\ \theta]\}^{(o)}, \tag{A.8}$$

where

$$\omega_D^{(o)} = (\bar{v}_D \cdot \nabla S)^{(o)} = \frac{q\epsilon}{\Omega R_o r m} (I_c + sI_s) \qquad (A.9)$$

with $I_c = (\cos\theta)^{(o)}$ and $I_s = (\theta \sin\theta)^{(o)}$. In the limit of concentric circular magnetic surfaces, I_c and I_s are simple to evaluate and yield

$$I_c(y^2) = [2E(y^2)/K(y^2)] - 1; \quad I_s(y^2) = 4[E(y^2)/K(y^2)] + 4(y^2 - 1); \quad (A.10)$$

where $2y^2 = 1 + (R/r)(1 - \Lambda)$, $K(y^2)$ and $E(y^2)$ are elliptic integrals of the first and second kind, respectively, and the pitch angle variable Λ is defined below Eq.(13). For trapped particles, $0 < y^2 < 1$, and $I_c + sI_s \approx 1$ in the deeply trapped limit $y^2 \to 0$. Adopting Eq.(A.10), we have to exclude relatively high beta plasmas ($\epsilon_o \beta_p \sim 1$) and highly elongated flux surfaces, where the departure from the result in Eq.(A.10) becomes significant [47].

In order to reduce Eq.(A.8) further, we use $\hat{\xi}_r \approx$ const and $\hat{\xi}_\theta \approx -i\hat{\xi}_r$, as $\nabla \cdot \bar{\xi}_\perp = O(\xi_\perp/R_o)$ in the outer region. Since $\kappa_r \approx -(\cos\theta)/R$, and $\kappa_\theta \approx (\sin\theta)/R_o$, we find

$$(\bar{\xi}_\perp \cdot \bar{\kappa}) \exp[i(q-1)\theta] \approx - (\hat{\xi}_r/R_o)(\cos q\theta) \qquad (A.11)$$

where odd terms in θ, which are annihilated once the average along the particle orbit is taken, have been disregarded. Using (A.11) in (A.8) and inserting the result into (A.3), Eq.(12) in the text is recovered.

The phases of f^{ad} and f^{nad} differ by a factor $i(R-S)\theta = i(q-1)\theta$, that is

$$f^{ad} = \hat{f}^{ad}(r,\epsilon)\exp(-i\omega t + iR) \qquad (A.12)$$

$$f^{nad} = \hat{f}^{nad}(r,\epsilon,\Lambda)\exp(-i\omega t + iS) \qquad (A.13)$$

Using corresponding definitions for $\tilde{\sigma} \equiv \tilde{p}_{\perp} + \tilde{p}_{||}$ we obtain

$$\left.\begin{matrix}\hat{\sigma}^{ad} \\ \hat{\sigma}^{nad}\end{matrix}\right\} = 2\pi \left(\frac{2}{m}\right)^{3/2} \int_{H_L}^{H} \frac{(1 - \Lambda/2H)d\Lambda}{H^2(1 - \Lambda/H)^{1/2}} \int_0^{\infty} d\epsilon\, \epsilon^{3/2} \left\{\begin{matrix}\hat{f}^{ad}(r,\epsilon) \\ \hat{f}^{nad}(r,\epsilon,\Lambda)\end{matrix}\right. \tag{A.14}$$

$H(r,\theta) = B_o/B$, B_o is the magnetic field strength on axis, $H_L = 0$ for the adiabatic term, and $H_L = H_{min} = H(r,\pi) \simeq 1-r/R$ for the nonadiabatic term. We observe that $\hat{\sigma}^{nad}(r,\theta)$ is an even function of θ such that in magnitude $|\partial\hat{\sigma}^{nad}/\partial\theta| \sim |\hat{\sigma}^{nad}|$. On the other hand $\hat{\sigma}^{ad}$ does not depend on θ to leading order in ϵ_o, since the equilibrium distribution function is assumed isotropic.

Now we set $\lambda_K = \lambda_K^{ad} + \lambda_K^{nad}$, where

$$\left.\begin{matrix}\lambda_K^{ad} \\ \lambda_K^{nad}\end{matrix}\right\} = -\frac{4\pi^2 i}{B_p^2 s_o \xi_o} \int_o^{r_o} dr r^2 \int_{-\pi}^{\pi} \frac{d\theta}{2\pi}\, \bar{e}_{||} \times \bar{\kappa} \cdot \left\{\begin{matrix}\nabla[\,\hat{\sigma}^{ad} \exp(iR)]\exp(-iR) \\ \nabla[\,\hat{\sigma}^{nad} \exp(iS)]\exp(-iR)\end{matrix}\right. , \tag{A.15}$$

To leading order in ϵ_o, $\bar{e}_{||} \times \bar{\kappa} \cdot \nabla\hat{\sigma}^{ad}$ is odd in θ and therefore does not contribute to the integral. Since $\bar{e}_{||} \times \bar{\kappa} \cdot \nabla R = (i/rR_o)\cos\theta$, we find

$$\lambda_K^{ad} \simeq \frac{2\pi}{B_p^2 s_o \xi_o R_o} \int_o^{r_o} r dr \int_{-\pi}^{\pi} d\theta\, \hat{\sigma}^{ad} \cos\theta \tag{A.16}$$

To leading order $\hat{\sigma}^{ad}$ is independent of θ and thus the integral (A.16) vanishes. More generally, λ_K^{ad} is negligible when $\partial\hat{\sigma}^{ad}/\partial\theta \sim \epsilon_o\hat{\sigma}^{ad}$, which holds for moderately anisotropic equilibria with $p_{\perp} \sim p_{||}$. Thus, $\lambda_K = \lambda_K^{nad}$.

To calculate λ_K^{nad} we write

$$ir^2(\bar{e}_{||}\times\bar{\kappa}\cdot\nabla S)\hat{\sigma}^{nad}\exp[i(1-q)\theta] =$$

$$= \frac{ir}{R_o}\hat{\sigma}^{nad}_q\,(\cos\theta + s\theta\sin\theta)\cos[(1-q)\theta] + \text{odd terms} \qquad (A.17)$$

and

$$r^2(\bar{e}_{||}\times\bar{\kappa}\cdot\nabla\hat{\sigma}^{nad})\exp[i(1-q)\theta] =$$

$$= ir^2\left(\kappa_r\frac{\partial\hat{\sigma}^{nad}}{r\partial\theta} - \kappa_\theta\frac{\partial\hat{\sigma}^{nad}}{\partial r}\right)\sin[(1-q)\theta] + \text{odd terms} \qquad (A.18)$$

and integrate by parts the terms involving $\partial\hat{\sigma}^{nad}/\partial\theta$ and $\partial\hat{\sigma}^{nad}/\partial r$. After straightforward algebra we arrive at

$$\lambda_K^{nad} = \frac{2\pi}{B_p^2 s_o R_o \xi_o}\int_o^{r_o} rdr\int_{-\pi}^{\pi} d\theta\;\hat{\sigma}^{nad}\cos(q\theta) \qquad (A.19)$$

Now we substitute $\hat{\sigma}^{nad}$ from Eq.(A.14) into Eq.(A.19). Using

$$\int_{-\pi}^{\pi} d\theta\int_{H_{min}}^{H} d\Lambda = \int_{H_{min}}^{H_{max}} d\Lambda\int_{-\theta_o}^{\theta_o} d\theta \qquad (A.20)$$

where $H_{max} = H(r,\theta=0)$ and $\theta_o(\Lambda)$ is the magnetic turning angle of a trapped particle orbit, we find

$$\lambda_K = \lambda_K^{nad} = \frac{2\sqrt{2}\pi^3}{B_p^2 s}\left(\frac{r_o}{R_o}\right)^{3/2}\left(\frac{2}{m}\right)^{3/2}\int_0^1 x^{1/2}dx\int_{H_{min}}^{H_{max}} d\Lambda\ I_q^2(x,\Lambda)I_o(x,\Lambda)$$

$$\times\int_o^\infty d\epsilon\epsilon^{5/2}\frac{\partial F_o}{\partial\epsilon}\frac{\omega-\omega_*^T}{\omega-\omega_D^{(0)}} \qquad (A.21)$$

where $x \equiv r/r_o$, $I_q(x,\Lambda) = [\cos(q\theta)]^{(0)}$, and $I_o(x,\Lambda) = (2r/R_o)^{1/2}\int_{-\theta_o}^{\theta_o}(d\theta/2\pi)$ $(1-\Lambda/H)^{-1/2}$.

In the limit of concentric circular magnetic surfaces, $I_o = 2K(y^2)/\pi$, reducing to $I_o \approx 1$ for deeply trapped particles.

Using the distribution function (22) with ϵ_c = const, neglecting terms of order $\epsilon_c/\epsilon_\alpha$, and noticing that $\omega/\omega_*^T \lesssim \omega_D^{(0)}/\omega_*^T \sim \epsilon_o$ for isotropic distributions, Eq.(A.21) can be recast in the form given by Eq.(22) in the text, where

$$\beta_{p\alpha} = -\frac{8\pi}{B_p^2(r_o)}\int_0^1 dx\, x^{3/2} I_\beta(x)\frac{dp_\alpha}{dx}\ , \qquad (A.22)$$

$$I_\beta(x) = \frac{3\pi}{8\epsilon_o x q(x)}\int_{H_{min}}^{H_{max}} d\Lambda\ \frac{I_q^2 I_o}{I_c + sI_s}\ , \qquad (A.23)$$

$$\Lambda_K(\hat{\omega}) = -\sqrt{2}/2\ [1 + \hat{\omega}\Phi(\hat{\omega})] \qquad (A.24)$$

$$\Phi(\hat{\omega}) = -\frac{\int_0^1 \frac{dx x^{1/2}}{q(x)} \frac{dp_\alpha}{dx} \int_{H_{min}}^{H_{max}} d\Lambda \frac{I_q^2 I_o}{I_c + sI_s} G(x,\Lambda,\hat{\omega})}{\int_0^1 \frac{dx x^{1/2}}{q(x)} \frac{dp_\alpha}{dx} \int_{H_{min}}^{H_{max}} d\Lambda \frac{I_q^2 I_o}{I_c + sI_s}} \qquad (A.25)$$

and

$$G(x,\Lambda,\hat{\omega}) = (1 + 2\chi\epsilon_c/3\epsilon_\alpha)^{-1} \int_0^1 \frac{\hat{\epsilon}^{3/2}}{\hat{\epsilon}_c^{3/2} + \hat{\epsilon}^{3/2}} \frac{d\hat{\epsilon}}{\hat{\omega} - (\hat{\epsilon}q/x)(I_c + sI_s)} \qquad (A.26)$$

with $\hat{\omega} = \omega/\bar{\omega}_{D\alpha}$ and $\hat{\epsilon} \equiv \epsilon/\epsilon_\alpha$. The Λ-integrals in Eqs.(A.23) and (A.25) are extended to the trapped particle population only. The energy integral (A.26) can be solved analytically in terms of logarithms and arcotangents, leaving the radial and pitch angle integrations to be performed numerically. A simplification of Eqs.(A.22)-(A.26) is obtained when (1-q) and s are small. Then, apart from corrections, $I_q \approx I_c$, $I_\beta \approx 1$ (using $\int_0^1 dy^2 [2E(y^2)-K(y^2)] = 2/3$), and $\beta_{p\alpha}$ reduces to Eq.(23) in the text. The function $\Lambda_K(\hat{\omega})$ depends weakly on plasma parameters. The most significant dependence is on the magnetic shear through the term $I_c + sI_s$ to which $\omega_{D\alpha}^{(o)}$ is proportional. This dependence is illustrated by the examples in Fig.17.

REFERENCES

[1] Ya. I. Kolesnichenko, Nucl. Fus. 20, 727 (1980)

[2] R.B. White, M.S. Chance, J.L. Johnson, H.E. Mynick, F.W. Perkins and A.H. Reiman, in Plasma Physics and Controlled Nuclear Fusion Research 1988 (IAEA, Nice, 1989), in press.

[3] B. Coppi and F. Pegoraro, Ann. Phys. (NY) 134, 376 (1981).

[4] K.T. Tsang and D.J. Sigmar, Nucl. Fus. 21, 1227 (1981).

[5] M.N. Rosenbluth, S.T. Tsai, J.W. van Dam, M.G. Engquist, Phys. Rev. Lett. 51, 1867 (1983).

[6] J. Weiland and L. Chen, Phys. Fluids 28, 1358 (1985).

[7] G. Rewoldt, Phys. Fluids 32, 3727 (1988).

[8] D. Campbell, D.F.H. Start, J.A. Wesson, D.V. Bartlett, V.P. Bhatnagar, M. Bures, J.G. Cordey, G.A. Cottrell, P.A. Dupperex, A.W. Edwards, C.D. Challis, G. Gormezano, C.W. Gowers, R.S. Granetz, H. Hamnén, T. Hellsten, J. Jacquinot, E. Lazzaro, P.J. Lomas, N. Lopes Cardozo, P. Mantica, J.A. Snipes, D. Stork, P.E. Stott, P.R. Thomas, E. Thompson, K. Thomsen and G. Tonetti, Phys. Rev. Lett. 60, 2148 (1988).

[9] G. McGuire, R. Goldston, M. Bell, M. Bitter, K. Bol, K. Brau, D. Buchenauer, T. Crowley, S. Davis, F. Dylla, H. Eubank, H. Fishman, R. Fonck, B. Grek, R. Grimm, R. Hawryluk, H. Hsuan, R. Hulse, R. Izzo, R. Kaita, S. Kaye, H. Kugel, D. Johnson, J. Manickam, D. Manos, D. Mansfield, E. Mazzucato, R. McCann, D. McCune, D. Monticello, R. Motley, D. Mueller, K. Oasa, M. Okabayashi, K. Owens, W. Park, M. Reusch, N. Sauthoff, G. Schmidt, S. Sesnic, J. Strachan, C. Surko, R. Slusher, H., Takahashi, F. Tenney, P. Thomas, H. Towner, J. Valley and R. White, Phys. Rev. Lett. 50, 891 (1983).

[10] W.W. Heidbrink, K. Bol, D. Buchenauer, R. Fonck, G. Gammel, K. Ida, R. Kaita, S. Kaye, H. Kugel, B. LeBlanc, W. Morris, M. Okabayashi, E. Powell, S. Sesnic and H. Takahashi, Phys. Rev. Lett. 57, 835 (1986).

[11] A.W. Morris, E.D. Fredrickson, K.M. McGuire, M.G. Bell, M.S. Chance, R.J. Goldston, R. Kaita, J. Manickam, S.S. Medley, N. Pomphrey, S.D. Scott, M.C. Zarnstorff, in Proc. of the 14th European Conf. on Controlled Fusion and Plasma Heating (EPS, Madrid, 1987), Vol. IID, Part 1, p.189.

[12] M.F.F. Nave, E. Joffrin, F. Pegoraro, F. Porcelli, P. Smeulders and K. Thomsen, in Proc. of the 16th European Conf. on Controlled Fusion and Plasma Heating (EPS, Venice, 1989), Vol.13B, Part II, p.505.

[13] B. Coppi, R.J. Hastie, S. Migliuolo, F. Pegoraro and F. Porcelli, Phys. Lett. A., 132, 267 (1988).

[14] B. Coppi and F. Porcelli, Phys. Rev. Lett. 57, 2272 (1986).

[15] L. Chen, R.B. White and M.N. Rosenbluth, Phys. Rev. Lett. 52, 1122 (1984).

[16] G. Ara, B. Basu, B. Coppi, G. Laval, M.N. Rosenbluth and B.V. Waddell, An. Phys. (NY) 112, 443 (1978).

[17] B. Coppi, R. Galvão, R. Pellat, M.N. Rosenbluth and P. Rutherford, Fiz. Plazmy 6, 961 (1976) [Sov. J. Plasma Phys. 2, 533 (1976)].

[18] M.N. Bussac, R. Pellat, D. Edery and J.L. Soulé, Phys. Rev. Lett. 35, 1638 (1975).

[19] J.W. Connor and R.J. Hastie, Culham Laboratory Report CLM-M-106 (1977).

[20] F. Pegoraro, F. Porcelli, B. Coppi, P. Detragiache and S. Migliuolo, in Plasma Physics and Controlled Nuclear Fusion Research 1988 (IAEA, Nice, 1989), Paper CN-50/D-4-6, in press.

[21] B. Coppi and F. Porcelli, Fusion Technology 13, 447 (1988).

[22] F. Pegoraro and T.J. Schep, Phys. Fluids 30, 3506 (1987).

[23] Chen Yan-Ping, R.J. Hastie, Ke Fu-Jiu, Cai Shi-Dong, L. Chen, Acta Physica Sinica 37, 546 (1988).

[24] F. Porcelli, B. Coppi, S. Migliuolo, Bull. Am. Phys. Soc. 32, 1770 (1987).

[25] F. Porcelli and F. Pegoraro, in Proc. of the II European Fusion Theory Meeting (Varenna, 1987), paper P48.

[26] R.B. White, P.H. Rutherford, P. Colestock and M.N. Bussac, Phys. Rev. Lett. 60, 2038 (1988); R.B. White, M.N. Bussac and F. Romanelli, Phys. Rev. Lett. 62, 539 (1989).

[27] Y.Z. Zhang, H.L. Berk, S.M. Mahajan and H.V. Wong, Bull. Am. Phys. Soc. 33, 2074 (1988), paper 8I6.

[28] F. Pegoraro, F. Porcelli and T.J. Schep, Phys. Fluids B1, 364 (1989).

[29] F. Pegoraro, F. Porcelli, T.J. Schep, B. Coppi and S. Migliuolo, in Proc. of the 1989 Sherwood Theory Conference (San Antonio, TX, 1989), Paper 2D35, in press.

[30] B. Coppi, S. Migliuolo and F. Porcelli, Phys. Fluids 31, 1630 (1988).

[31] J.B. Taylor and R.J. Hastie, Phys. Fluids 8, 323 (1965).

[32] B. Coppi, S. Cowley, P. Detragiache, R.S. Kulsrud and F. Pegoraro, Phys. Fluids 29, 4060 (1986).

[33] A.B. Mikhailovskii, Fiz. Plazmy 9, 326 (1983) [Sov. J. Plasma Phys. 9, 198 (1984)].

[34] B.N. Kuvshinov and A.B. Mikhailovskii, Fiz. Plazmy 13, 915 (1987) [Sov. J. Plasma Phys. 13, 527 (1987)].

[35] M.N. Bussac, D. Edery, R. Pellat and J.L. Soulé, in Plasma Physics and Controlled Nuclear Fusion Research 1976 (IAEA, Berchtesgaden, 1977), Vol.1, p.607.

[36] B. Coppi, R. Englade, S. Migliuolo, F. Porcelli and L. Sugiyama, in Plasma Physics and Controlled Nuclear Fusion Research 1986 (IAEA, Kyoto, 1987), Vol.3, p.397.

[37] J.F. Drake, T.M. Antonsen Jr., A.B. Hassam and N.T. Gladd, Phys. Fluids 26, 2509 (1983).

[38] S.C. Cowley, R.M. Kulsrud and T.S. Hahm, Phys. Fluids 29, 3230 (1986).

[39] R.J. Hastie, T.C. Hender, B.A. Carreras, L.A. Charlton and J.A. Holmes, Phys. Fluids 30, 1756 (1987).

[40] F. Porcelli and S. Migliuolo, Phys. Fluids 29, 1741 (1986).

[41] M. Kotschenreuther, in Proc. of the 1987 Sherwood Theory Conference (San Diego, CA), Paper 2D10.

[42] T.S. Hahm, Phys. Fluids 31, 3709 (1988).

[43] F. Pegoraro, F. Porcelli, B. Coppi and S. Migliuolo, in Proc. of the 16th Europ. Conf. on Controlled Fusion and Plasma Physics (EPS, Venice, 1989), Vol.13B, Part I, p.275.

[44] Y.A. Kolesnichenko and A.D. Fursa, Fiz. Plazmy 1, 806 (1975) [Sov. J. Plasma Phys. 1, 442 (1975)].

[45] R. Bickerton and the JET Team, in Plasma Physics and Controlled Nuclear Fusion Research 1988 (IAEA, Nice, 1989), in press.

[46] D. Campbell, et al., in Proc. of the 15th Europ. Conf. on Controlled Fusion and Plasma Physics (EPS, Dubrovnik, 1988), Vol.12B, Part I, p.377.

[47] C.Z. Cheng, private communication.

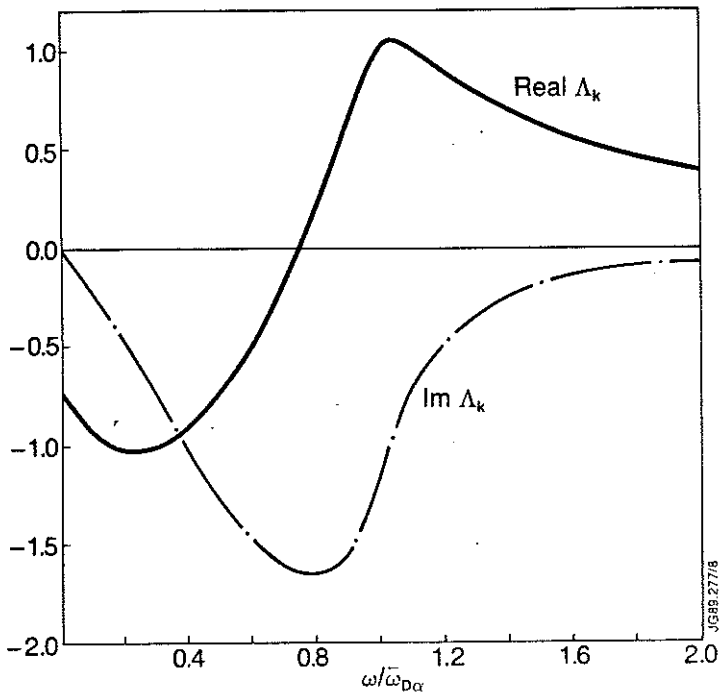

Fig. 1 Real and imaginary parts of $\Lambda_K(\omega/\bar{\omega}_{D\alpha}) \equiv s_0\, \beta_{p\alpha}^{-1}\, \epsilon_o^{-3/2}\, \lambda_K(\omega/\bar{\omega}_{D\alpha})$, where λ_K is the alpha particle contribution to the dispersion relation [see Eq.(21)]. A parabolic q profile inside the $q=1$ surface with $q(0)=0.8$ has been assumed.

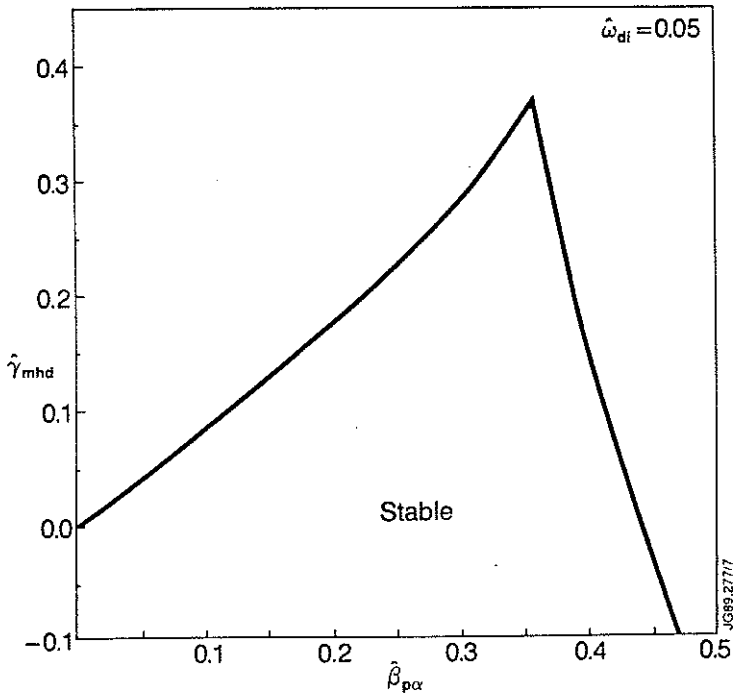

Fig. 2 Marginal stability curve in the $(\hat{\gamma}_{mhd}, \hat{\beta}_{p\alpha})$ plane, for a constant value of the normalised diamagnetic frequency $\hat{\omega}_{di}=0.05$ and the same q profile as in Fig. 1. The stable domain lies below the curve. The normalised quantities $\hat{\gamma}_{mhd}$, $\hat{\beta}_{p\alpha}$ and $\hat{\omega}_{di}$ are defined in Eqs.(28), (29), and below Eq.(27), respectively.

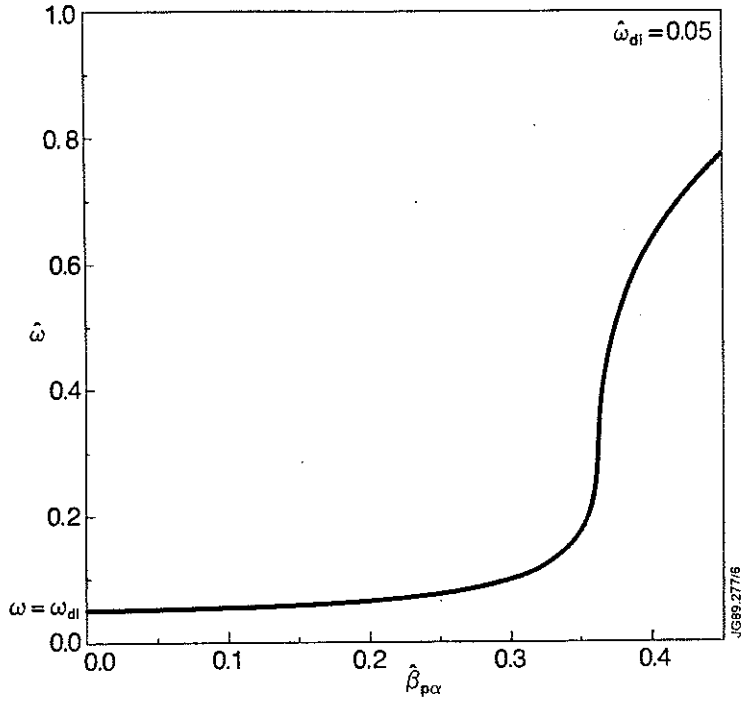

Fig. 3 Normalised mode frequency $\hat{\omega} \equiv \omega/\bar{\omega}_{D\alpha}$ as a function of $\hat{\beta}_{p\alpha}$ along the marginal stability curve of Fig. 2.

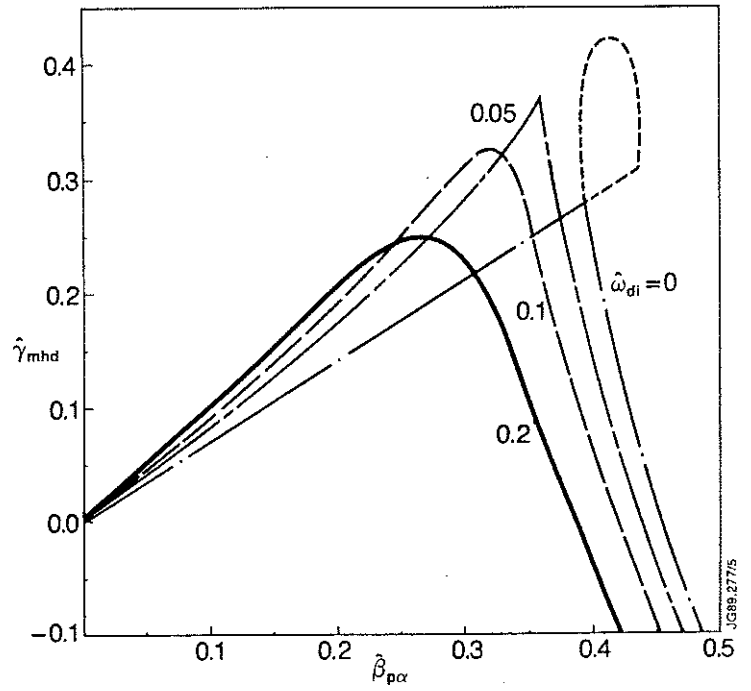

Fig. 4 Marginal stability curves in the $(\hat{\gamma}_{mhd}, \hat{\beta}_{p\alpha})$ plane for different values of $\hat{\omega}_{di}$ indicated in the figure. For $\hat{\omega}_{di}=0$, the curve forms a loop, inside which two different unstable solutions of Eqs.(26)-(27) are found.

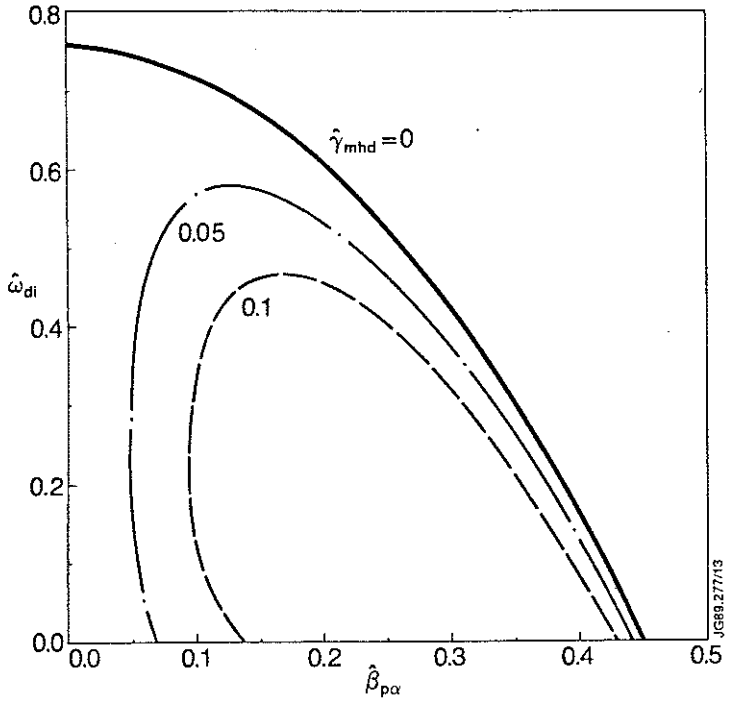

Fig. 5 Marginal stability curves in the $(\hat{\omega}_{di}, \hat{\beta}_{p\alpha})$ plane for different values of $\hat{\gamma}_{mhd}$ indicated in the figure. The corresponding stable domain lies below each curve.

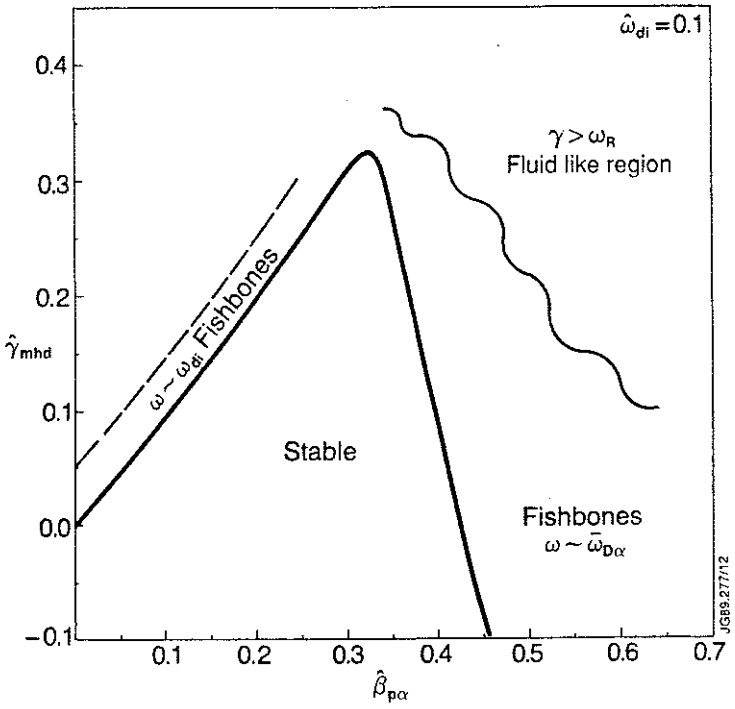

Fig. 6 Stable domain and unstable regimes in the $(\hat{\gamma}_{mhd}, \hat{\beta}_{p\alpha})$ plane, for $\hat{\omega}_{di}=0.1$.

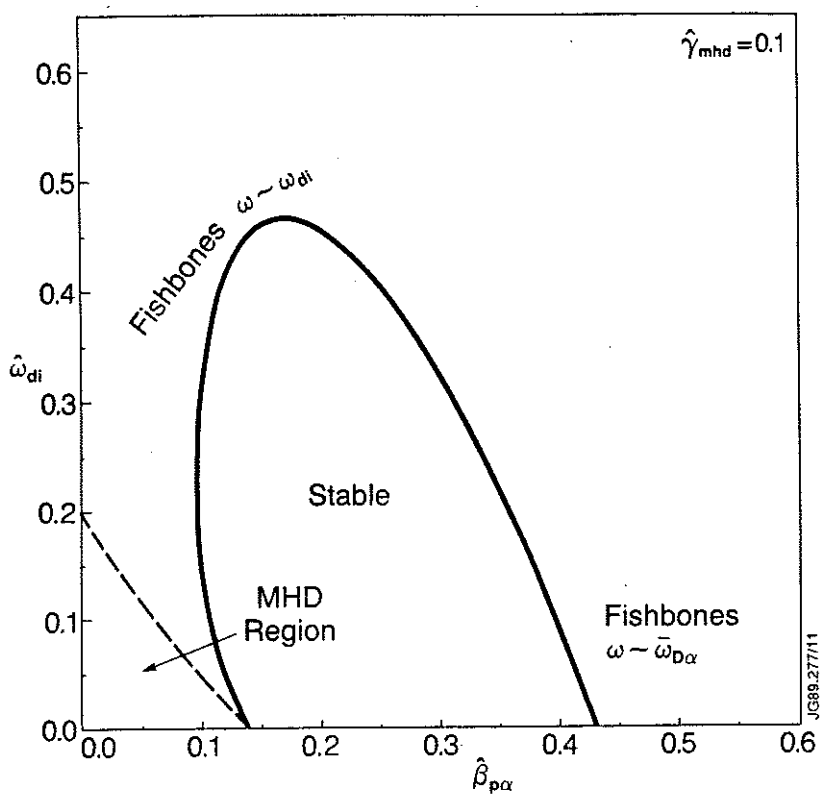

Fig. 7 Stable domain and unstable regimes in the $(\hat{\omega}_{di}, \hat{\beta}_{p\alpha})$ plane, for fixed value $\hat{\gamma}_{mhd}=0.1$.

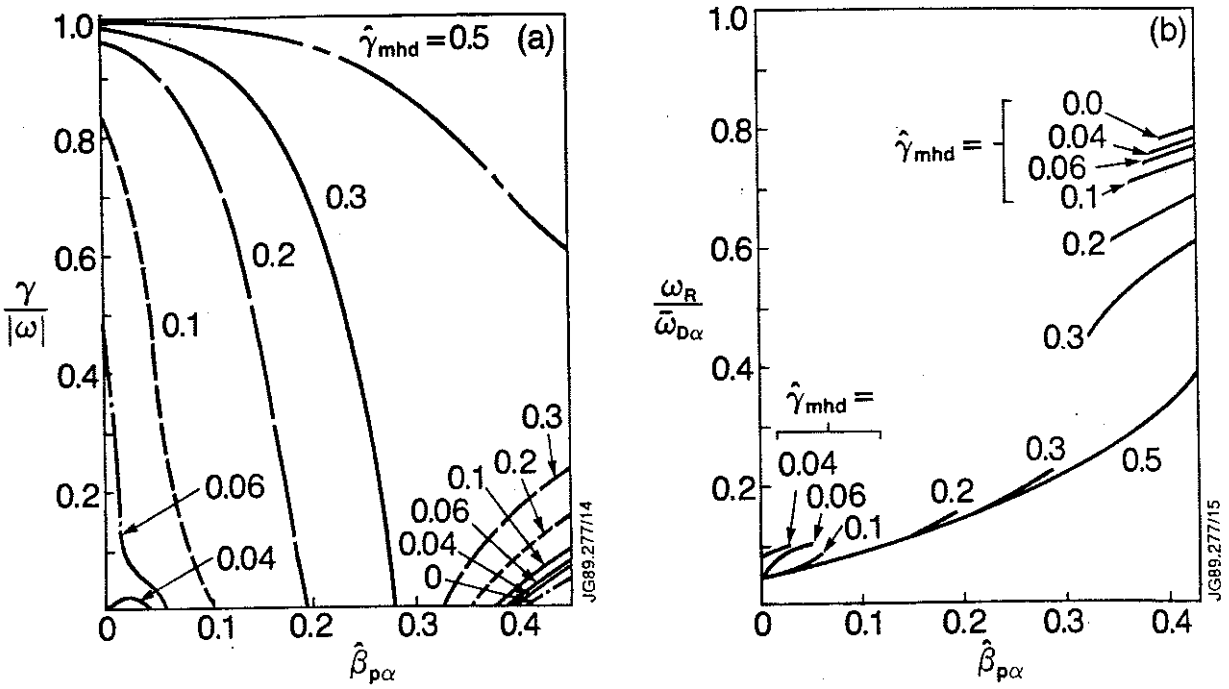

Fig. 8 Graphs of (a) the ratio $\gamma/|\omega|$, and of (b) the normalised oscillation frequency, $\omega_R/\bar{\omega}_{D\alpha}$, of the higher frequency solution of the dispersion relation (2), as a function of $\hat{\beta}_{p\alpha}$ for different values of $\hat{\gamma}_{mhd}$ (indictaed in the figure); $\hat{\omega}_{di}=0.1$ for all curves.

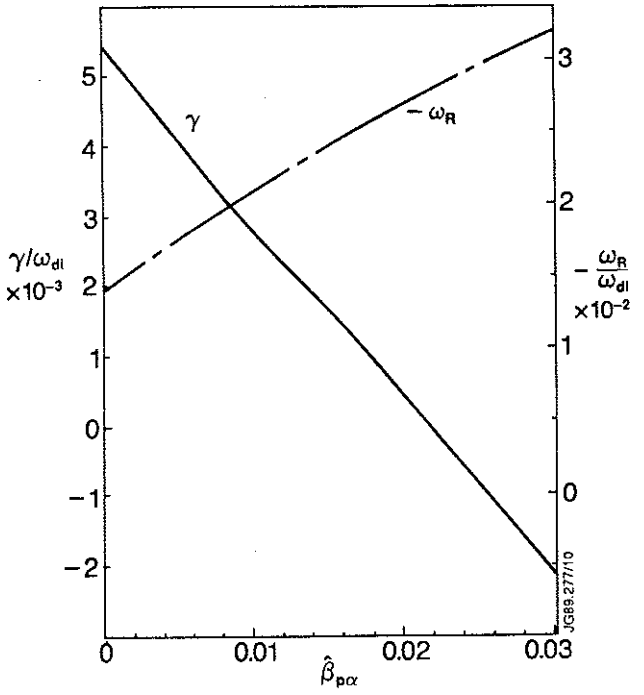

Fig. 9 Graphs of the normalised growth rate, γ/ω_{di} (solid line) and of the normalised oscillation frequency $-\omega_R/\omega_{di}$ (dashed line) of the lower frequency solution of the relevant dispersion relation, in the presence of resistivity $\eta_\parallel$ and transverse viscosity $\mu_\perp$ (see Ref.40), as a function of $\hat{\beta}_{p\alpha}$. The values of the relevant parameters are: $\lambda_H=0$; $\omega_{di}/\bar{\omega}_{D\alpha}=0.1$, $\Omega_{di}\equiv|\omega_{di}|/(\omega_A\ \epsilon_\eta^{1/3})=4$, $\epsilon_\eta=1.25\times10^{-7}$, and $D\equiv\epsilon_\mu/\epsilon_\eta=0.08$. Here, $\epsilon_\eta\equiv\eta_\parallel\ s_o^2\ c^2/(4\pi r_o^2\ \omega_A)$, and $\epsilon_\mu\equiv s_o^2\ \mu_\perp/m_i n_{io} r_o^2$. Note that $D\simeq(3/10)(T_e\ m_i/T_i\ m_e)_o^{1/2}\ \beta_{eo}$, with $\beta_{eo}=8\pi n_e(r_o)\ T_e(r_o)/B^2$.

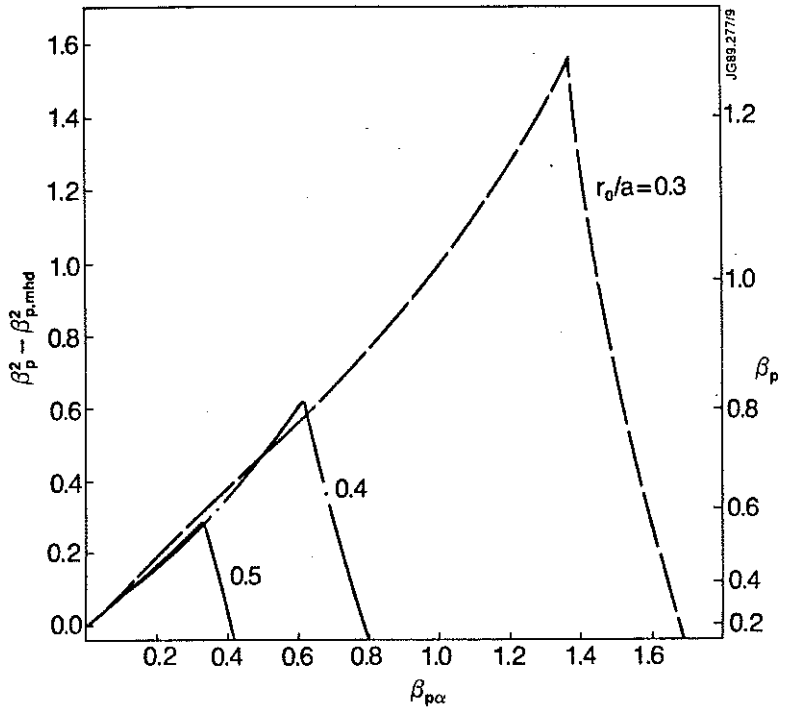

Fig. 10 Marginal stability curves in the $(\Delta\beta_p^2, \beta_{p\alpha})$ plane, where $\Delta\beta_p^2 = \beta_p^2 - \beta_{p,mhd}^2$, for the following parameter values: $\omega_{di}/\bar{\omega}_{D\alpha} = 0.05$; $\bar{\omega}_{D\alpha}/\omega_A = 0.2$; $s_o = 0.6$, $a/R_o = 1/3$, and different values of r_o/a indicated near each curve. At $r_o/a = 0.3$, we have taken $\omega_{di}/\bar{\omega}_{D\alpha} = 0.05$; and $\bar{\omega}_{D\alpha}/\omega_A = 0.2$, their radial dependence being given below Eq.(44). The corresponding values of β_p assuming $\beta_{p,mhd} = 0.2$ are indicated on the scale to the right.

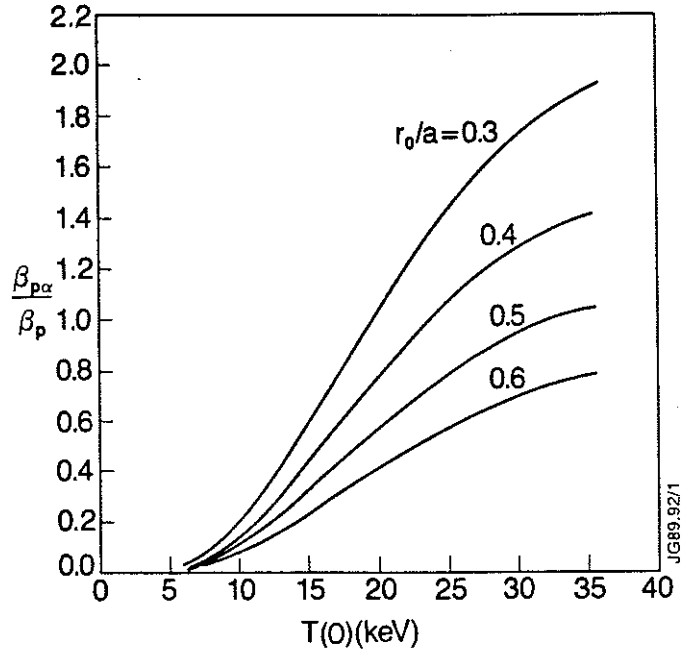

Fig. 11 The ratio $\beta_{p\alpha}/\beta_p$ as a function of the central plasma temperature $T(0)$, for different values of r_o/a indicated near each curve, and for the following values of the parabolic profile exponents [see Eq.(46)]: $\sigma = 6$; $\sigma_n = 1$; $\sigma_T = 3/2$..

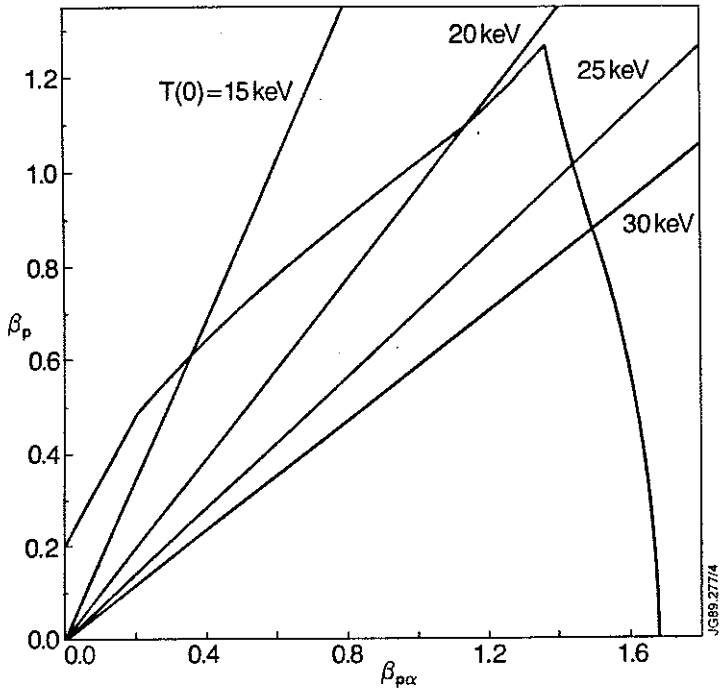

Fig. 12 Marginal stability curve in the (β_p, $\beta_{p\alpha}$) plane, assuming $\beta_{p,mhd}=0.2$ and the following parameter values: $\omega_{di}/\tilde{\omega}_{D\alpha}=0.05$; $\tilde{\omega}_{D\alpha}/\omega_A=0.2$; $s_o=0.6$; and $r_o/R_o=0.1$. The straight lines correspond to different ratios of $\beta_p/\beta_{p\alpha}$ for different values of the central temperature $T(0)$, and the following parabolic profile exponents [see Eq.(46)]: $\sigma=6$; $\sigma_n=1$, $\sigma_T=3/2$.

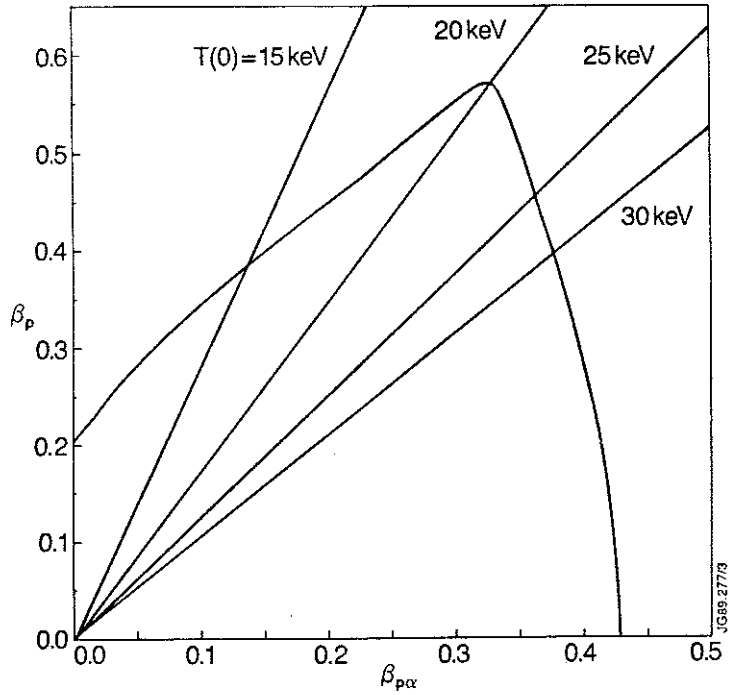

Fig. 13 Equivalent of Fig. 12, for $r_o/R_o=0.17$, $\omega_{di}/\tilde{\omega}_{D\alpha}=0.076$, and $\tilde{\omega}_{D\alpha}/\omega_A=0.11$, assuming the radial scaling $\omega_{di}/\tilde{\omega}_{D\alpha}\propto(r_o/a)\,(1-r_o^2/a^2)^{1/2}$, $\tilde{\omega}_{D\alpha}/\omega_A\propto(a/r_o)\,(1-r_o^2/a^2)^{1/2}$, and $a/R_o=1/3$. Note change of scale compared with previous figure.

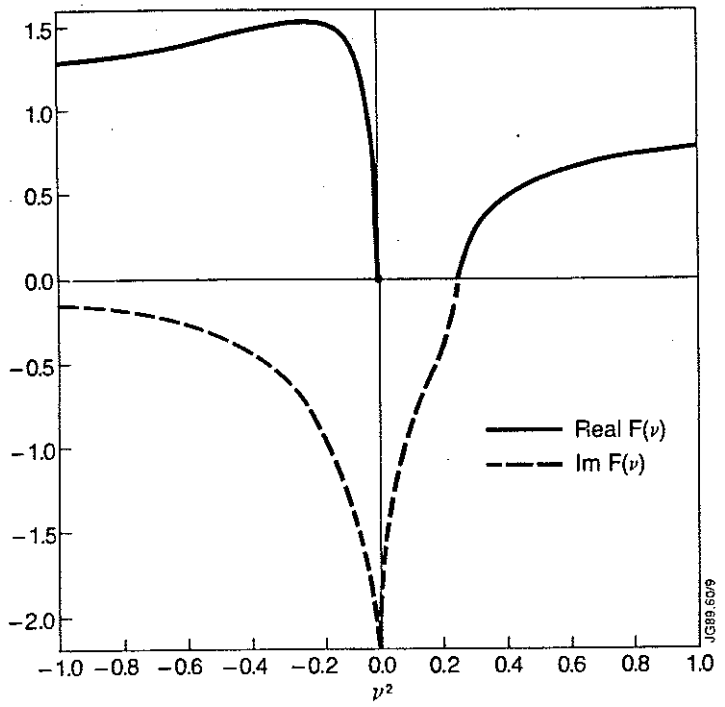

Fig. 14 Real and imaginary parts of the function $F(\nu)$, defined in Eq.(49), versus real ν^2, defined in Eq.(50).

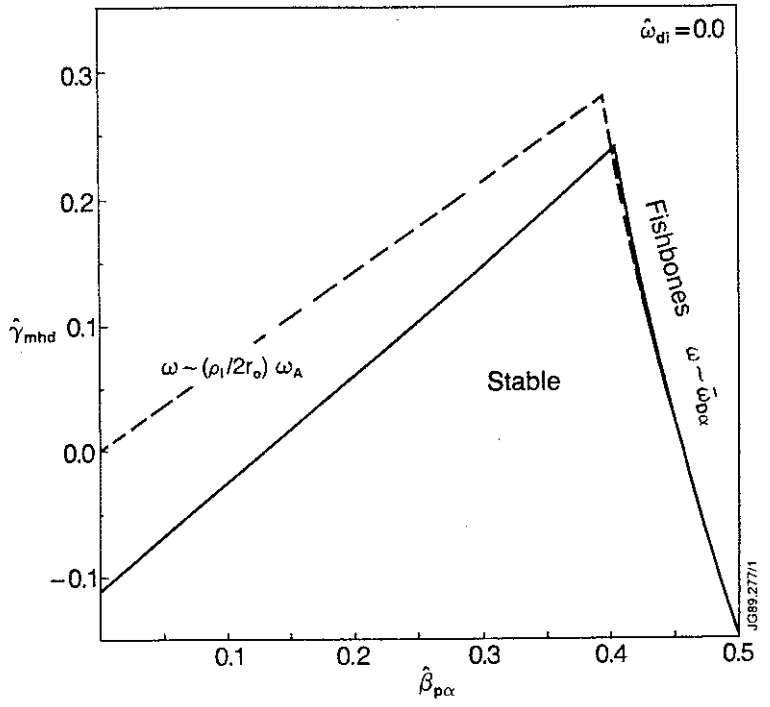

Fig. 15 Marginal stability curve in the $(\hat{\gamma}_{mhd}, \hat{\beta}_{p\alpha})$ plane, for $\hat{\omega}_{di}=0$ and $\hat{\rho}_i=0.1$ [see definition in Eq.(51)].

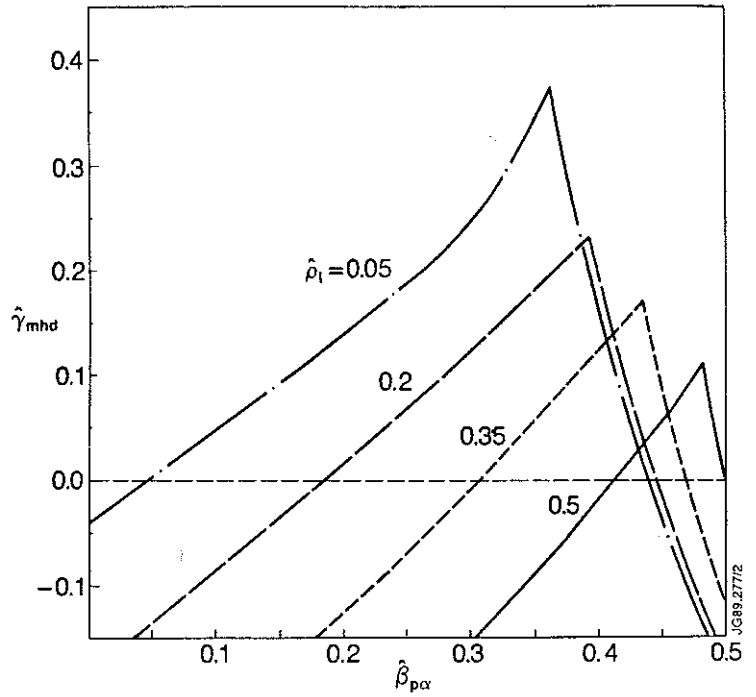

Fig. 16 Marginal stability curves in the $(\hat{\gamma}_{mhd}, \hat{\beta}_{p\alpha})$ plane, for $\hat{\omega}_{di} = 0.05$ and different values of $\hat{\rho}_i$ indicated near each curve.

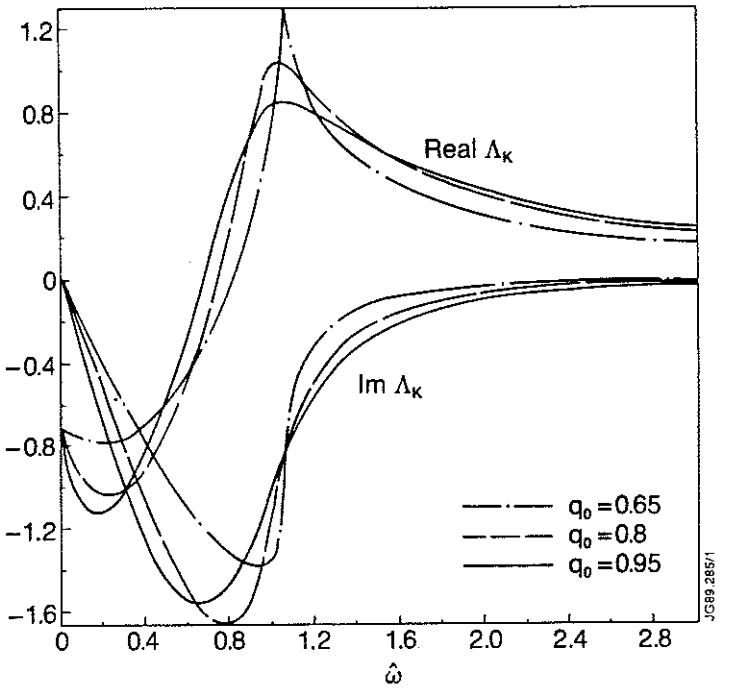

Fig. 17 Real and imaginary parts of $\Lambda_K(\hat{\omega})$ for different values of $q(0)$. A parabolic q profile inside the $q=1$ surface has been assumed.